Scientific Research Publishing

American Journal of Computational Mathematics, 2020, 10, 529-558
https://www.scirp.org/journal/ajcm
ISSN Online: 2161-1211
ISSN Print: 2161-1203

Third Order Adjoint Sensitivity and Uncertainty Analysis of an OECD/NEA Reactor Physics Benchmark: II. Computed Sensitivities

Ruixian Fang, Dan Gabriel Cacuci*

Center for Nuclear Science and Energy, Department of Mechanical Engineering, University of South Carolina, Columbia, SC, USA
Email: fangr@cec.sc.edu, *cacuci@cec.sc.edu

How to cite this paper: Fang, R.X. and Cacuci, D.G. (2020) Third Order Adjoint Sensitivity and Uncertainty Analysis of an OECD/NEA Reactor Physics Benchmark: II. Computed Sensitivities. *American Journal of Computational Mathematics*, **10**, 529-558.
https://doi.org/10.4236/ajcm.2020.104030

Received: October 16, 2020
Accepted: December 4, 2020
Published: December 7, 2020

Abstract

This work presents the results of the exact computation of $(180)^3 = 5{,}832{,}000$ third-order mixed sensitivities of the leakage response of a polyethylene-reflected plutonium (PERP) experimental benchmark with respect to the benchmark's 180 microscopic total cross sections. This computation was made possible by applying the Third-Order Adjoint Sensitivity Analysis Methodology developed by Cacuci. The numerical results obtained in this work revealed that many of the 3rd-order sensitivities are significantly larger than their corresponding 1st- and 2nd-order ones, which is contrary to the widely held belief that higher-order sensitivities are all much smaller and hence less important than the first-order ones, for reactor physics systems. In particular, the largest 3rd-order relative sensitivity is the mixed sensitivity $S^{(3)}\left(\sigma_{t,1}^{g=30},\sigma_{t,6}^{g'=30},\sigma_{t,6}^{g''=30}\right)=-1.88\times10^{5}$ of the PERP leakage response with respect to the lowest energy-group (30) total cross sections of ^{1}H ("isotope 6") and ^{239}Pu ("isotope 1"). These two isotopes are shown in this work to be the two most important parameters affecting the PERP benchmark's leakage response. By comparison, the largest 1st-order sensitivity is that of the PERP leakage response with respect to the lowest energy-group total cross section of isotope ^{1}H, having the value $S^{(1)}\left(\sigma_{t,6}^{30}\right)=-9.366$, while the largest 2nd-order sensitivity is $S^{(2)}\left(\sigma_{t,6}^{30},\sigma_{t,6}^{30}\right)=429.6$. The 3rd-order sensitivity analysis presented in this work is the first ever such analysis in the field of reactor physics. The consequences of the results presented in this work on the uncertainty analysis of the PERP benchmark's leakage response will be presented in a subsequent work.

Keywords

Polyethylene-Reflected Plutonium Sphere, 1st-Order Sensitivities, 2nd-Order Sensitivities, 3rd-Order Sensitivities, Third Order Adjoint Sensitivity Analysis, Microscopic Total Cross Sections

1. Introduction

The accompanying Part I [1] has reported the exact mathematical expressions of the 3rd-order sensitivities of the leakage response of the OECD/NEA subcritical polyethylene-reflected plutonium (acronym: PERP) metal fundamental physics benchmark [2] with respect to the benchmark's group-averaged microscopic total cross sections. The exact mathematical expressions of these 3rd-order sensitivities were derived by applying the general Third-Order Adjoint Sensitivity Analysis Methodology conceived by Cacuci [3]. This work will present the numerical results obtained by using the formulas derived in [1] for the $(180)^3$ third-order mixed sensitivities of the PERP's leakage response with respect to the benchmark's 180 group-averaged microscopic total cross sections. The numerical results obtained for the 3rd-order relative sensitivities are then compared with the corresponding 1st- and 2nd-order ones, which have been computed and reported in [4] [5]. The magnitudes and distributions of the 3rd-order mixed relative sensitivities will be illustrated in 3D plots.

This work is organized as follows: Section 2 reports the numerical results for the 180 third-order "unmixed" sensitivities of the PERP's leakage response with respect to the microscopic total cross sections, comparing them with the corresponding 1st- and 2nd-order sensitivities. Section 3 presents the numerical results for the mixed third-order sensitivities, highlighting the magnitudes and distributions for the largest of these. Section 4 summarizes and highlights the significance of the pioneering results obtained in this work.

2. Numerical Results for Third-Order Unmixed Sensitivities of the PERP Leakage Response to Total Cross Sections

The characteristics of the OECD/NEA polyethylene-reflected plutonium (acronym: PERP) metal sphere benchmark for subcritical neutron and gamma measurements have been detailed in Part I [1] and in [4] [5]. The mathematical expression of the 3rd-order mixed sensitivities $\partial^3 L(\boldsymbol{\alpha})/\partial t_j \partial t_k \partial t_\ell$, $j,k,\ell = 1,\cdots,J_{\sigma t}$ of the PERP leakage response with respect to the group-averaged microscopic total cross sections has been derived in the accompanying Part I [1] and is reproduced in the Appendix, for convenient reference. In this Section, the computed values of the 3rd-order *unmixed* relative sensitivities, *i.e.*, $S^{(3)}\left(\sigma_{t,j}^g, \sigma_{t,j}^g, \sigma_{t,j}^g\right) \triangleq \left(\partial^3 L/\partial\sigma_{t,j}^g \partial\sigma_{t,j}^g \partial\sigma_{t,j}^g\right)\left(\sigma_{t,j}^g \sigma_{t,j}^g \sigma_{t,j}^g / L\right)$, $g = 1,\cdots,30$, $j = 1,\cdots,6$, are compared to the corresponding values of the 1st-order relative sensitivities

$S^{(1)}\left(\sigma_{t,j}^{g}\right) \triangleq \left(\partial L/\partial\sigma_{t,j}^{g}\right)\left(\sigma_{t,j}^{g}/L\right)$ for $g=1,\cdots,30,\ j=1,\cdots,6$, as well as to the corresponding values of the 2nd-order unmixed relative sensitivities $S^{(2)}\left(\sigma_{t,j}^{g},\sigma_{t,j}^{g}\right) \triangleq \left(\partial^{2} L/\partial\sigma_{t,j}^{g}\partial\sigma_{t,j}^{g}\right)\left(\sigma_{t,j}^{g}\sigma_{t,j}^{g}/L\right), g=1,\cdots,30,\ j=1,\cdots,6$. The term "unmixed" denotes the sensitivity of the PERP leakage response with respect to the same parameter. The numerical values for the 1st-order and 2nd-order unmixed relative sensitivities of PERP leakage response with respect to the benchmark's total cross sections have been computed and documented in [4].

Tables 1-6 present side-by-side comparisons of the unmixed sensitivities of order 1-3 for each of the six isotopes contained in the PERP benchmark.

Table 1 presents the comparison of 1st-order, 2nd-order and 3rd-order unmixed relative sensitivities for isotope 1 (^{239}Pu), for all energy groups $g=1,\cdots,30$. This comparison indicates that, for the same energy group, the absolute values of the 3rd-order relative sensitivities are generally much larger than the corresponding values of both the 1st- and 2nd-order sensitivities. Specifically, for the energy groups $g=6,\cdots,26$ and $g=30$, the values of the 3rd-order relative sensitivities are around 1.6 - 6.6 times of the corresponding values of the 2nd-order sensitivities, and are larger than the corresponding values of the 1st-order sensitivities by factors ranging from 2.0 to 29.7 times. The largest values (shown in bold in the table) for the 1st-order, 2nd-order and 3rd-order relative sensitivities all occur for

Table 1. Comparison of the 1st-order, 2nd-order and 3rd-order unmixed relative sensitivities, $S^{(1)}\left(\sigma_{t,1}^{g}\right), S^{(2)}\left(\sigma_{t,1}^{g},\sigma_{t,1}^{g}\right), S^{(3)}\left(\sigma_{t,1}^{g},\sigma_{t,1}^{g},\sigma_{t,1}^{g}\right), g=1,\cdots,30$ for isotope 1 (^{239}Pu) of the PERP benchmark.

g	1st-Order	2nd-Order	3rd-Order	g	1st-Order	2nd-Order	3rd-Order
1	−0.0003	0.0003	−0.0003	16	−0.779	3.487	−23.10
2	−0.0007	0.0005	−0.0005	17	−0.364	1.578	−10.07
3	−0.0019	0.0015	−0.0015	18	−0.227	0.995	−6.428
4	−0.009	0.007	−0.008	19	−0.181	0.789	−5.063
5	−0.046	0.043	−0.054	20	−0.155	0.601	−3.431
6	−0.135	0.162	−0.267	21	−0.137	0.479	−2.480
7	−0.790	1.987	−7.294	22	−0.099	0.297	−1.313
8	−0.726	1.768	−6.270	23	−0.081	0.205	−0.777
9	−0.843	2.205	−8.454	24	−0.051	0.123	−0.438
10	−0.845	2.177	−8.247	25	−0.060	0.138	−0.473
11	−0.775	1.879	−6.691	26	−0.063	0.158	−0.581
12	**−1.320**	**4.586**	**−23.71**	27	−0.017	0.022	−0.039
13	−1.154	4.039	−20.96	28	−0.003	0.002	−0.0017
14	−0.952	3.435	−18.29	29	−0.035	0.072	−0.226
15	−0.690	2.487	−13.18	30	−0.461	1.353	−5.980

Table 2. Comparison of the 1st-order, 2nd-order and 3rd-order unmixed relative sensitivities, $S^{(1)}\left(\sigma_{t,2}^{g}\right), S^{(2)}\left(\sigma_{t,2}^{g},\sigma_{t,2}^{g}\right), S^{(3)}\left(\sigma_{t,2}^{g},\sigma_{t,2}^{g},\sigma_{t,2}^{g}\right), g=1,\cdots,30$ for isotope 2 (^{240}Pu).

g	1st-Order	2nd-Order	3rd-Order	g	1st-Order	2nd-Order	3rd-Order
1	-2.060×10^{-5}	1.052×10^{-6}	-6.857×10^{-8}	16	-4.864×10^{-2}	1.052×10^{-6}	-5.606×10^{-3}
2	-4.117×10^{-5}	2.089×10^{-6}	-1.358×10^{-7}	17	-2.236×10^{-2}	2.089×10^{-6}	-2.328×10^{-3}
3	-1.192×10^{-4}	6.055×10^{-6}	-3.948×10^{-7}	18	-1.358×10^{-2}	6.055×10^{-6}	-1.383×10^{-3}
4	-5.638×10^{-4}	2.947×10^{-5}	-1.994×10^{-6}	19	-1.021×10^{-2}	2.947×10^{-5}	-9.170×10^{-4}
5	-2.894×10^{-3}	1.730×10^{-4}	-1.370×10^{-5}	20	-8.914×10^{-3}	1.730×10^{-4}	-6.590×10^{-4}
6	-8.513×10^{-3}	6.485×10^{-4}	-6.744×10^{-5}	21	-6.716×10^{-3}	6.485×10^{-4}	-2.947×10^{-4}
7	-4.958×10^{-2}	7.836×10^{-3}	-1.806×10^{-3}	22	-4.676×10^{-3}	7.836×10^{-3}	-1.364×10^{-4}
8	-4.574×10^{-2}	7.026×10^{-3}	-1.571×10^{-3}	23	-7.458×10^{-3}	7.026×10^{-3}	-6.187×10^{-4}
9	-5.318×10^{-2}	8.769×10^{-3}	-2.120×10^{-3}	24	-4.371×10^{-3}	8.769×10^{-3}	-2.703×10^{-4}
10	-5.345×10^{-2}	8.711×10^{-3}	-2.087×10^{-3}	25	-8.131×10^{-4}	8.711×10^{-3}	-1.170×10^{-6}
11	-4.909×10^{-2}	7.547×10^{-3}	-1.703×10^{-3}	26	-9.171×10^{-4}	7.547×10^{-3}	-1.776×10^{-6}
12	-8.364×10^{-2}	1.842×10^{-2}	-6.032×10^{-3}	27	-1.862×10^{-2}	1.842×10^{-2}	-4.965×10^{-2}
13	-7.145×10^{-2}	1.548×10^{-2}	-4.974×10^{-3}	28	-9.671×10^{-3}	1.548×10^{-2}	-3.722×10^{-2}
14	-5.953×10^{-2}	1.342×10^{-2}	-4.466×10^{-3}	29	-1.364×10^{-4}	1.342×10^{-2}	-1.385×10^{-8}
15	-4.267×10^{-2}	9.506×10^{-3}	-3.114×10^{-3}	30	-7.909×10^{-3}	9.506×10^{-3}	-3.016×10^{-5}

Table 3. Comparison of the 1st-order, 2nd-order and 3rd-order unmixed relative sensitivities, $S^{(1)}\left(\sigma_{t,3}^{g}\right), S^{(2)}\left(\sigma_{t,3}^{g},\sigma_{t,3}^{g}\right), S^{(3)}\left(\sigma_{t,3}^{g},\sigma_{t,3}^{g},\sigma_{t,3}^{g}\right), g=1,\cdots,30$ for isotope 3 (^{69}Ga).

g	1st-Order	2nd-Order	3rd-Order	g	1st-Order	2nd-Order	3rd-Order
1	-9.214×10^{-7}	2.104×10^{-9}	-6.132×10^{-12}	16	-2.551×10^{-3}	3.733×10^{-5}	-8.089×10^{-7}
2	-1.974×10^{-6}	4.804×10^{-9}	-1.497×10^{-11}	17	-1.262×10^{-3}	1.893×10^{-5}	-4.187×10^{-7}
3	-6.012×10^{-6}	1.541×10^{-8}	-5.068×10^{-11}	18	-8.411×10^{-4}	1.371×10^{-5}	-3.289×10^{-7}
4	-3.036×10^{-5}	8.545×10^{-8}	-3.114×10^{-10}	19	-8.605×10^{-4}	1.790×10^{-5}	-5.485×10^{-7}
5	-1.587×10^{-4}	5.204×10^{-7}	-2.260×10^{-9}	20	-6.458×10^{-4}	1.050×10^{-5}	-2.506×10^{-7}
6	-4.353×10^{-4}	1.696×10^{-6}	-9.018×10^{-9}	21	-3.919×10^{-4}	3.949×10^{-6}	-5.856×10^{-8}
7	-2.107×10^{-3}	1.415×10^{-5}	-1.386×10^{-7}	22	-1.489×10^{-4}	6.668×10^{-7}	-4.408×10^{-9}
8	-1.717×10^{-3}	9.897×10^{-6}	-8.307×10^{-8}	23	-1.104×10^{-4}	3.859×10^{-7}	-2.008×10^{-9}
9	-1.912×10^{-3}	1.133×10^{-5}	-9.845×10^{-8}	24	-3.199×10^{-5}	4.778×10^{-8}	-1.059×10^{-10}
10	-1.956×10^{-3}	1.166×10^{-5}	-1.022×10^{-7}	25	-1.726×10^{-5}	1.136×10^{-8}	-1.118×10^{-11}
11	-1.943×10^{-3}	1.182×10^{-5}	-1.055×10^{-7}	26	-5.147×10^{-5}	1.046×10^{-7}	-3.139×10^{-10}
12	-3.756×10^{-3}	3.714×10^{-5}	-5.464×10^{-7}	27	-2.586×10^{-5}	4.825×10^{-8}	-1.331×10^{-10}
13	-3.522×10^{-3}	3.762×10^{-5}	-5.957×10^{-7}	28	-8.496×10^{-7}	1.192×10^{-10}	-2.523×10^{-14}
14	-2.987×10^{-3}	3.371×10^{-5}	-5.624×10^{-7}	29	-6.754×10^{-7}	2.747×10^{-11}	-1.682×10^{-15}
15	-2.182×10^{-3}	2.485×10^{-5}	-4.163×10^{-7}	30	-2.542×10^{-5}	4.111×10^{-9}	-1.002×10^{-12}

Table 4. Comparison of the 1st-order, 2nd-order and 3rd-order unmixed relative sensitivities, $S^{(1)}\left(\sigma_{t,4}^{g}\right), S^{(2)}\left(\sigma_{t,4}^{g}, \sigma_{t,4}^{g}\right), S^{(3)}\left(\sigma_{t,4}^{g}, \sigma_{t,4}^{g}, \sigma_{t,4}^{g}\right), g = 1, \cdots, 30$ for isotope 4 (^{71}Ga).

g	1st-Order	2nd-Order	3rd-Order	g	1st-Order	2nd-Order	3rd-Order
1	-6.266×10^{-7}	9.730×10^{-10}	-1.928×10^{-12}	16	-1.662×10^{-3}	1.585×10^{-5}	-2.237×10^{-7}
2	-1.345×10^{-6}	2.230×10^{-9}	-4.734×10^{-12}	17	-8.176×10^{-4}	7.950×10^{-6}	-1.139×10^{-7}
3	-4.103×10^{-6}	7.176×10^{-9}	-1.611×10^{-11}	18	-5.318×10^{-4}	5.479×10^{-6}	-8.310×10^{-8}
4	-2.069×10^{-5}	3.967×10^{-8}	-9.849×10^{-11}	19	-4.939×10^{-4}	5.898×10^{-6}	-1.037×10^{-7}
5	-1.072×10^{-4}	2.374×10^{-7}	-6.966×10^{-10}	20	-3.976×10^{-4}	3.979×10^{-6}	-5.847×10^{-8}
6	-2.906×10^{-4}	7.557×10^{-7}	-2.683×10^{-9}	21	-2.344×10^{-4}	1.413×10^{-6}	-1.253×10^{-8}
7	-1.397×10^{-3}	6.218×10^{-6}	-4.037×10^{-8}	22	-2.170×10^{-3}	1.416×10^{-4}	-1.364×10^{-5}
8	-1.149×10^{-3}	4.436×10^{-6}	-2.492×10^{-8}	23	-1.337×10^{-4}	5.659×10^{-7}	-3.568×10^{-9}
9	-1.295×10^{-3}	5.202×10^{-6}	-3.063×10^{-8}	24	-1.322×10^{-5}	8.156×10^{-9}	-7.470×10^{-12}
10	-1.327×10^{-3}	5.368×10^{-6}	-3.192×10^{-8}	25	-7.518×10^{-6}	2.154×10^{-9}	-9.232×10^{-13}
11	-1.318×10^{-3}	5.439×10^{-6}	-3.296×10^{-8}	26	-2.313×10^{-5}	2.112×10^{-8}	-2.848×10^{-11}
12	-2.549×10^{-3}	1.710×10^{-5}	-1.707×10^{-7}	27	-1.201×10^{-5}	1.041×10^{-8}	-1.333×10^{-11}
13	-2.375×10^{-3}	1.711×10^{-5}	-1.828×10^{-7}	28	-4.131×10^{-7}	2.818×10^{-11}	-2.901×10^{-15}
14	-2.005×10^{-3}	1.521×10^{-5}	-1.705×10^{-7}	29	-3.512×10^{-7}	7.429×10^{-12}	-2.365×10^{-16}
15	-1.481×10^{-3}	1.145×10^{-5}	-1.302×10^{-7}	30	-1.665×10^{-5}	1.764×10^{-9}	-2.815×10^{-13}

Table 5. Comparison of the 1st-order, 2nd-order and 3rd-order unmixed relative sensitivities, $S^{(1)}\left(\sigma_{t,5}^{g}\right), S^{(2)}\left(\sigma_{t,5}^{g}, \sigma_{t,5}^{g}\right), S^{(3)}\left(\sigma_{t,5}^{g}, \sigma_{t,5}^{g}, \sigma_{t,5}^{g}\right), g = 1, \cdots, 30$ for isotope 5 (C).

g	1st-Order	2nd-Order	3rd-Order	g	1st-Order	2nd-Order	3rd-Order
1	-9.992×10^{-6}	1.066×10^{-6}	1.038×10^{-7}	16	-2.074×10^{-1}	1.415×10^{-1}	-1.429×10^{-1}
2	-2.017×10^{-5}	2.185×10^{-6}	4.236×10^{-8}	17	-1.665×10^{-1}	9.779×10^{-2}	-8.554×10^{-2}
3	-6.373×10^{-5}	7.901×10^{-6}	-3.833×10^{-7}	18	-1.439×10^{-1}	7.678×10^{-2}	-6.114×10^{-2}
4	-2.996×10^{-4}	3.873×10^{-5}	-3.872×10^{-6}	19	-1.310×10^{-1}	6.625×10^{-2}	-5.004×10^{-2}
5	-1.597×10^{-3}	2.359×10^{-4}	-3.370×10^{-5}	20	-1.212×10^{-1}	5.905×10^{-2}	-4.297×10^{-2}
6	-4.403×10^{-3}	6.521×10^{-4}	-1.175×10^{-4}	21	-1.129×10^{-1}	5.347×10^{-2}	-3.780×10^{-2}
7	-3.698×10^{-2}	9.376×10^{-3}	-3.113×10^{-3}	22	-1.036×10^{-1}	4.747×10^{-2}	-3.247×10^{-2}
8	-4.631×10^{-2}	1.447×10^{-2}	-5.744×10^{-3}	23	-9.589×10^{-2}	4.280×10^{-2}	-2.851×10^{-2}
9	-4.502×10^{-2}	1.114×10^{-2}	-3.553×10^{-3}	24	-8.693×10^{-2}	3.756×10^{-2}	-2.422×10^{-2}
10	-5.135×10^{-2}	1.368×10^{-2}	-4.754×10^{-3}	25	-8.213×10^{-2}	3.496×10^{-2}	-2.220×10^{-2}
11	-5.645×10^{-2}	1.633×10^{-2}	-6.262×10^{-3}	26	-7.550×10^{-2}	3.142×10^{-2}	-1.949×10^{-2}
12	-1.345×10^{-1}	6.055×10^{-2}	-3.799×10^{-2}	27	-6.727×10^{-2}	2.701×10^{-2}	-1.617×10^{-2}
13	-1.529×10^{-1}	8.249×10^{-2}	-6.342×10^{-2}	28	-6.224×10^{-2}	2.437×10^{-2}	-1.422×10^{-2}
14	-1.504×10^{-1}	8.573×10^{-2}	-7.064×10^{-2}	29	-5.995×10^{-2}	2.298×10^{-2}	-1.312×10^{-2}
15	-1.299×10^{-1}	6.928×10^{-2}	-5.391×10^{-2}	30	-7.847×10^{-1}	3.016×10^{0}	-1.745×10^{1}

Table 6. Comparison of the 1st-order, 2nd-order and 3rd-order unmixed relative sensitivities, $S^{(1)}\left(\sigma_{t,6}^{g}\right), S^{(2)}\left(\sigma_{t,6}^{g},\sigma_{t,6}^{g}\right), S^{(3)}\left(\sigma_{t,6}^{g},\sigma_{t,6}^{g},\sigma_{t,6}^{g}\right), g=1,\cdots,30$ for isotope 6 (^{1}H).

g	1st-Order	2nd-Order	3rd-Order	g	1st-Order	2nd-Order	3rd-Order
1	-8.471×10^{-6}	7.636×10^{-7}	6.322×10^{-8}	16	-1.164×10^{0}	4.460×10^{0}	-2.530×10^{1}
2	-2.060×10^{-5}	2.280×10^{-6}	4.516×10^{-8}	17	-1.173×10^{0}	4.853×10^{0}	-2.991×10^{1}
3	-6.810×10^{-5}	9.021×10^{-6}	-4.677×10^{-7}	18	-1.141×10^{0}	4.828×10^{0}	-3.049×10^{1}
4	-3.932×10^{-4}	6.673×10^{-5}	-8.758×10^{-6}	19	-1.094×10^{0}	4.619×10^{0}	-2.913×10^{1}
5	-2.449×10^{-3}	5.549×10^{-4}	-1.216×10^{-4}	20	-1.033×10^{0}	4.284×10^{0}	-2.655×10^{1}
6	-9.342×10^{-3}	2.935×10^{-3}	-1.123×10^{-3}	21	**-9.692×10^{0}**	3.937×10^{0}	-2.388×10^{1}
7	-7.589×10^{-2}	3.949×10^{-2}	-2.690×10^{-2}	22	-8.917×10^{-1}	3.515×10^{0}	-2.069×10^{1}
8	-9.115×10^{-2}	5.604×10^{-2}	-4.380×10^{-2}	23	-8.262×10^{-1}	3.177×10^{0}	-1.823×10^{1}
9	-1.358×10^{-1}	1.014×10^{-1}	-9.758×10^{-2}	24	-7.495×10^{-1}	2.792×10^{0}	-1.552×10^{1}
10	-1.659×10^{-1}	1.428×10^{-1}	-1.604×10^{-1}	25	-7.087×10^{-1}	2.604×10^{0}	-1.427×10^{1}
11	-1.899×10^{-1}	1.849×10^{-1}	-2.385×10^{-1}	26	-6.529×10^{-1}	2.349×10^{0}	-1.260×10^{1}
12	-4.446×10^{-1}	6.620×10^{-1}	-1.373×10^{0}	27	-5.845×10^{-1}	2.039×10^{0}	-1.061×10^{1}
13	-5.266×10^{-1}	9.782×10^{-1}	-2.590×10^{0}	28	-5.474×10^{-1}	1.885×10^{0}	-9.678×10^{0}
14	-5.772×10^{-1}	1.262×10^{0}	-3.991×10^{0}	29	-5.439×10^{-1}	1.891×10^{0}	-9.800×10^{0}
15	-5.820×10^{-1}	1.391×10^{0}	-4.581×10^{0}	30	-9.366×10^{0}	**4.296×10^{2}**	**-2.966×10^{4}**

the 12th energy group, *i.e.*, $S^{(1)}\left(\sigma_{t,1}^{g=12}\right)=-1.32$, $S^{(2)}\left(\sigma_{t,1}^{g=12},\sigma_{t,1}^{g=12}\right)=4.586$ and $S^{(3)}\left(\sigma_{t,1}^{g=12},\sigma_{t,1}^{g=12},\sigma_{t,1}^{g=12}\right)=-23.71$. It is noteworthy that all of the 1st-order and 3rd-order unmixed relative sensitivities are negative, while all the unmixed 2nd-order ones are positive. A negative value for the 1st-order sensitivity signifies that an increase in the microscopic total cross section $\sigma_{t,1}^{g}$ will cause a decrease in the leakage L.

The results presented in Tables 2-4 indicate that all the 1st-, 2nd- and 3rd-order unmixed relative sensitivities for the isotopes 2, 3 and 4 (namely, ^{240}Pu, ^{69}Ga and ^{71}Ga), respectively, are very small (*i.e.*, in the order of 10^{-2} and less). For the same energy group of each isotope, the value of the 1st-order relative sensitivity is generally the largest, followed by the 2nd-order sensitivity, while the 3rd-order sensitivity is generally the smallest. For instance, for the same energy group of isotopes ^{69}Ga and ^{71}Ga, respectively, the values of the 1st-order relative sensitivities are ca. 2-3 orders of magnitudes greater than the corresponding values of the 2nd-order sensitivities, and ca. 4-5 orders of magnitudes greater than the corresponding values of the 3rd-order ones. Also, all of the 1st- and 3rd-order unmixed relative sensitivities that are presented in Tables 2-4 are negative, while all the 2nd-order unmixed relative sensitivities are positive.

As shown in Table 5, the values of the 1st-, 2nd- and 3rd-order unmixed relative sensitivities for isotope 5 (C) are mostly of the order of 10^{-1} or 10^{-2} (or less) for all energy groups, except for the lowest energy group (g = 30). For each energy group of g = 1 … 29, the 1st-order relative sensitivities are the largest, followed

by the 2nd-order and the 3rd-order sensitivities. Specifically, for these groups, the absolute values of the 1st-order relative sensitivities are ca. one order of magnitude greater than that of the corresponding 2nd-order sensitivities, while the 2nd-order sensitivities are generally 1 to 3 times greater than the corresponding 3rd-order ones. However, for the lowest group (g = 30), the 3rd-order relative sensitivity $S^{(3)}\left(\sigma_{t,5}^{g=30},\sigma_{t,5}^{g=30},\sigma_{t,5}^{g=30}\right)=-17.45$ has the largest absolute value, followed by the 2nd-order unmixed relative sensitivity $S^{(2)}\left(\sigma_{t,5}^{g=30},\sigma_{t,5}^{g=30}\right)=3.01$; the absolute value of the 1st-order relative sensitivity $S^{(1)}\left(\sigma_{t,5}^{g=30}\right)=-0.782$ is the smallest.

As shown in Table 6, many of the relative sensitivities for isotope 6 (^{1}H) have absolute values greater than 1.0, including 6 first-order sensitivities, 16 second-order unmixed sensitivities, and 18 third-order unmixed sensitivities. For energy groups g = 1 … 11, the 1st-order sensitivities are slightly larger (in absolute values) than the corresponding 2nd- and 3rd-order ones, but all are small. For energy groups g = 12 … 29, all of the 3rd-order unmixed relative sensitivities have absolute values greater than 1.0 and are significantly larger than the corresponding 1st- and 2nd-order ones. Depending on the specific energy group, the absolute values of the 3rd-order relative sensitivity are ca. 2 to 6 times larger than the corresponding 2nd-order ones and ca. 3 to 27 times larger than the values of the corresponding 1st-order sensitivities. The largest absolute values for all the 1st-, 2nd- and 3rd-order sensitivities are highlighted in bold digits in Table 6; they occur for the lowest-energy group (g = 30), where the 3rd-order sensitivity $S^{(3)}\left(\sigma_{t,6}^{g=30},\sigma_{t,6}^{g=30},\sigma_{t,6}^{g=30}\right)=-2.966\times10^{4}$ attains a very large absolute value; the 2nd-order sensitivity $S^{(2)}\left(\sigma_{t,6}^{g=30},\sigma_{t,6}^{g=30}\right)=4.283\times10^{2}$ is also the largest among the 2nd-order ones, while the 1st-order sensitivity $S^{(1)}\left(\sigma_{t,6}^{g=30}\right)=-9.338$ is only slightly smaller (in absolute value) than $S^{(1)}\left(\sigma_{t,6}^{g=21}\right)=-9.692$.

As indicated by the results presented in Tables 2-5, the 3rd-order relative sensitivities are all smaller than both the 1st-order and 2nd-order relative sensitivities for isotopes 2, 3, 4, and 5 (with one exception, for isotope 5 at g = 30). However, the results that are presented in Table 1 and Table 6 indicate that for isotope 1 (^{239}Pu) and isotope 6 (^{1}H), the 3rd-order relative sensitivities are generally larger than the corresponding 1st-order and 2nd-order relative sensitivities. For isotope 1 (^{239}Pu), the largest 3rd-order unmixed sensitivity is about 4 times larger than the corresponding 2nd-order relative sensitivity, and about 20 times larger than that of the corresponding 1st-order one. Notably for isotope 6 (^{1}H), the largest 3rd-order unmixed sensitivity is about 70 times larger than the corresponding 2nd-order relative sensitivity and is ca. 3000 times larger than the corresponding 1st-order one. The results presented in Tables 1-6 indicate that the 1st-order and 3rd-order unmixed relative sensitivities are negative while the 2nd-order unmixed relative sensitivities are all positive, for all the isotopes contained in the PERP sphere. The results in Tables 1-6 indicate that largest 1st-, 2nd- and 3rd-order sensitivities, and hence the most important consequential effects for the PERP benchmark's leakage response, arise from the microscopic total cross sections of isotopes ^{1}H and ^{239}Pu.

As indicated in [4], all the numerical values for the 1st-order and unmixed 2nd-order relative sensitivities in Tables 1-6 have been independently verified with the results being obtained from the central-difference estimates using forward PARTISN [6] computations in which the isotopic total cross section for each group was perturbed by small amounts, as needed for the respective finite-difference formulas. Similar verifications of the values obtained by using the 3rd-LASS were also performed in this work for 3rd-order unmixed relative sensitivities, which were alternatively computed using central-difference methods in conjunction with forward PARTISN [6] computations in which the isotopic total cross section for each group was perturbed by small amounts. The result of the verification of the largest sensitivities for isotope ^{239}Pu, which occurs in group 12, is presented in Table 7. Furthermore, Table 8 shows the verification of largest overall unmixed sensitivities of the PERP benchmark's leakage response to the microscopic total cross section, which occurs in group 30 of isotope ^{1}H. The results in both Table 7 and Table 8 provide confidence that the numerical solution of the 3rd-LASS is not only efficient but also very accurate.

3. Numerical Results for the Third-Order Mixed Sensitivities of the PERP Leakage Response to Total Cross Sections

The matrix of 3rd-order mixed relative sensitivities $\boldsymbol{S}^{(3)}\left(\sigma_{t,j}^{g},\sigma_{t,k}^{g'},\sigma_{t,l}^{g''}\right) \triangleq \left(\partial^{3}L/\partial\sigma_{t,j}^{g}\partial\sigma_{t,k}^{g'}\partial\sigma_{t,l}^{g''}\right)\left(\sigma_{t,j}^{g}\sigma_{t,k}^{g'}\sigma_{t,l}^{g''}/L\right),\ j,k,l=1,\cdots,6;g,g',g''=1,\cdots,30$ has dimensions $J_{\sigma t}\times J_{\sigma t}\times J_{\sigma t}\left(=180\times180\times180\right)$. To facilitate the presentation of its elements, the matrix $\boldsymbol{S}^{(3)}\left(\sigma_{t,j}^{g},\sigma_{t,k}^{g'},\sigma_{t,l}^{g''}\right)$ has been partitioned into $I\times I\times I=6\times6\times6=216$ submatrices, each of dimensions $G\times G\times G=30\times30\times30$. Because of symmetry of the 3rd-order sensitivities, only 56 of these 216 submatrices are district. For example, the values of the corresponding components of the following submatrices are identical: $\boldsymbol{S}^{(3)}\left(\sigma_{t,j=1}^{g},\sigma_{t,k=2}^{g'},\sigma_{t,l=3}^{g''}\right)$, $\boldsymbol{S}^{(3)}\left(\sigma_{t,j=1}^{g},\sigma_{t,k=3}^{g'},\sigma_{t,l=2}^{g''}\right)$, $\boldsymbol{S}^{(3)}\left(\sigma_{t,j=2}^{g},\sigma_{t,k=1}^{g'},\sigma_{t,l=3}^{g''}\right)$, $\boldsymbol{S}^{(3)}\left(\sigma_{t,j=2}^{g},\sigma_{t,k=3}^{g'},\sigma_{t,l=1}^{g''}\right)$, $\boldsymbol{S}^{(3)}\left(\sigma_{t,j=3}^{g},\sigma_{t,k=1}^{g'},\sigma_{t,l=2}^{g''}\right)$ and $\boldsymbol{S}^{(3)}\left(\sigma_{t,j=3}^{g},\sigma_{t,k=2}^{g'},\sigma_{t,l=1}^{g''}\right)$. Therefore, only the summary of the main features of each distinct submatrix are presented in Tables 9-14, in the following form: for a submatrix that comprises elements with relative sensitivities having absolute values greater than 1.0, the total number of such elements are counted and shown in the table. Otherwise, if the relative sensitivities of all elements of a submatrix have values lying in the interval (−1.0, 1.0), only the element having the largest absolute value in the submatrix, together with the phase-space coordinates of that element, are listed in the respective Table.

For the submatrices which comprise components with absolute values less than 1.0, as shown in Tables 9-14, most of the largest absolute values are of the order of 10^{-2} or smaller, particularly the mixed 3rd-order relative sensitivities involving the microscopic total cross sections of isotopes ^{240}Pu, ^{69}Ga, and ^{71}Ga.

Table 7. Verification of the 1st-, 2nd- and 3rd-order unmixed relative sensitivities, $S^{(1)}\left(\sigma_{t,1}^{g=12}\right), S^{(2)}\left(\sigma_{t,1}^{g=12},\sigma_{t,1}^{g=12}\right), S^{(3)}\left(\sigma_{t,1}^{g=12},\sigma_{t,1}^{g=12},\sigma_{t,1}^{g=12}\right), g=12$ for isotope 1 (^{239}Pu) of the PERP benchmark.

Unmixed Relative Sensitivities	1st-Order	2nd-Order	3rd-Order
Computed results using adjoint functions (from Table 1)	−1.319	4.586	−23.78
Results using central-difference method	−1.320	4.649	−24.25

Table 8. Verification of the 1st-, 2nd- and 3rd-order unmixed relative sensitivities, $S^{(1)}\left(\sigma_{t,6}^{g=30}\right), S^{(2)}\left(\sigma_{t,6}^{g=30},\sigma_{t,6}^{g=30}\right), S^{(3)}\left(\sigma_{t,6}^{g=30},\sigma_{t,6}^{g=30},\sigma_{t,6}^{g=30}\right), g=30$ for isotope 6 (^{1}H) of the PERP benchmark.

Unmixed Relative Sensitivities	1st-Order	2nd-Order	3rd-Order
Computed results using adjoint functions (from Table 6)	−9.366	429.6	-2.966×10^{4}
Results using central-difference method	−9.369	430.6	-3.017×10^{4}

Table 9. Summary presentation of the distinct submatrices within the matrix $\boldsymbol{S}^{(3)}\left(\sigma_{t,j=1}^{g},\sigma_{t,k}^{g'},\sigma_{t,l}^{g''}\right), j=1; k,l=1,\cdots,6; g,g',g''=1,\cdots,30$.

Isotopes	$l=1$ (^{239}Pu)	$l=2$ (^{240}Pu)	$l=3$ (^{69}Ga)	$l=4$ (^{71}Ga)	$l=5$ (C)	$l=6$ (^{1}H)
$k=1$ (^{239}Pu)	$\boldsymbol{S}^{(3)}\left(\sigma_{t,1}^{g},\sigma_{t,1}^{g'},\sigma_{t,1}^{g''}\right)$ 2027 elements with absolute values > 1.0	$\boldsymbol{S}^{(3)}\left(\sigma_{t,1}^{g},\sigma_{t,1}^{g'},\sigma_{t,2}^{g''}\right)$ 4 elements with absolute values > 1.0	$\boldsymbol{S}^{(3)}\left(\sigma_{t,1}^{g},\sigma_{t,1}^{g'},\sigma_{t,3}^{g''}\right)$ Min. value = -7.56×10^{-2} at $g=g'=g''=16$	$\boldsymbol{S}^{(3)}\left(\sigma_{t,1}^{g},\sigma_{t,1}^{g'},\sigma_{t,4}^{g''}\right)$ Min. value = -4.92×10^{-2} at $g=g'=g''=16$	$\boldsymbol{S}^{(3)}\left(\sigma_{t,1}^{g},\sigma_{t,1}^{g'},\sigma_{t,5}^{g''}\right)$ 188 elements with absolute values >1.0	$\boldsymbol{S}^{(3)}\left(\sigma_{t,1}^{g},\sigma_{t,1}^{g'},\sigma_{t,6}^{g''}\right)$ 3090 elements with absolute values >1.0
$k=2$ (^{240}Pu)		$\boldsymbol{S}^{(3)}\left(\sigma_{t,1}^{g},\sigma_{t,2}^{g'},\sigma_{t,2}^{g''}\right)$ Min. value = -9.52×10^{-2} at $g=g'=g''=12$	$\boldsymbol{S}^{(3)}\left(\sigma_{t,1}^{g},\sigma_{t,2}^{g'},\sigma_{t,3}^{g''}\right)$ Min. value = -4.71×10^{-3} at $g=g'=g''=16$	$\boldsymbol{S}^{(3)}\left(\sigma_{t,1}^{g},\sigma_{t,2}^{g'},\sigma_{t,4}^{g''}\right)$ Min. value = -3.07×10^{-3} at $g=g'=g''=16$	$\boldsymbol{S}^{(3)}\left(\sigma_{t,1}^{g},\sigma_{t,2}^{g'},\sigma_{t,5}^{g''}\right)$ Min. value = -5.25×10^{-1} at $g=g'=12, g''=30$	$\boldsymbol{S}^{(3)}\left(\sigma_{t,1}^{g},\sigma_{t,2}^{g'},\sigma_{t,6}^{g''}\right)$ 120 elements with absolute values > 1.0
$k=3$ (^{69}Ga)			$\boldsymbol{S}^{(3)}\left(\sigma_{t,1}^{g},\sigma_{t,3}^{g'},\sigma_{t,3}^{g''}\right)$ Min. value = -2.47×10^{-4} at $g=g'=g''=16$	$\boldsymbol{S}^{(3)}\left(\sigma_{t,1}^{g},\sigma_{t,3}^{g'},\sigma_{t,4}^{g''}\right)$ Min. value = -1.61×10^{-4} at $g=g'=g''=16$	$\boldsymbol{S}^{(3)}\left(\sigma_{t,1}^{g},\sigma_{t,3}^{g'},\sigma_{t,5}^{g''}\right)$ Min. value = -2.30×10^{-2} at $g=g'=12, g''=30$	$\boldsymbol{S}^{(3)}\left(\sigma_{t,1}^{g},\sigma_{t,3}^{g'},\sigma_{t,6}^{g''}\right)$ Min. value = -2.82×10^{-1} at $g=g'=12, g''=30$
$k=4$ (^{71}Ga)				$\boldsymbol{S}^{(3)}\left(\sigma_{t,1}^{g},\sigma_{t,4}^{g'},\sigma_{t,4}^{g''}\right)$ Min. value = -6.25×10^{-4} at $g=g'=g''=22$	$\boldsymbol{S}^{(3)}\left(\sigma_{t,1}^{g},\sigma_{t,4}^{g'},\sigma_{t,5}^{g''}\right)$ Min. value = -1.60×10^{-2} at $g=g'=12, g''=30$	$\boldsymbol{S}^{(3)}\left(\sigma_{t,1}^{g},\sigma_{t,4}^{g'},\sigma_{t,6}^{g''}\right)$ Min. value = -1.90×10^{-1} at $g=g'=12, g''=30$
$k=5$ (C)					$\boldsymbol{S}^{(3)}\left(\sigma_{t,1}^{g},\sigma_{t,5}^{g'},\sigma_{t,5}^{g''}\right)$ 817 elements with absolute value > 1.0	$\boldsymbol{S}^{(3)}\left(\sigma_{t,1}^{g},\sigma_{t,5}^{g'},\sigma_{t,6}^{g''}\right)$ 2013 elements with absolute values > 1.0
$k=6$ (^{1}H)						$\boldsymbol{S}^{(3)}\left(\sigma_{t,1}^{g},\sigma_{t,6}^{g'},\sigma_{t,6}^{g''}\right)$ 7998 elements with absolute values > 1.0

Table 10. Summary presentation of the distinct submatrices within the matrix $\boldsymbol{S}^{(3)}\left(\sigma_{t,j=2}^{g},\sigma_{t,k}^{g'},\sigma_{t,l}^{g''}\right), j=2; k,l=1,\cdots,6; g,g',g''=1,\cdots,30$.

Isotopes	$l=2$ (^{240}Pu)	$l=3$ (^{69}Ga)	$l=4$ (^{71}Ga)	$l=5$ (C)	$l=6$ (^{1}H)
$k=2$ (^{240}Pu)	$\boldsymbol{S}^{(3)}\left(\sigma_{t,2}^{g},\sigma_{t,2}^{g'},\sigma_{t,2}^{g''}\right)$ Min. value = -4.96×10^{-2} at $g=g'=g''=27$	$\boldsymbol{S}^{(3)}\left(\sigma_{t,2}^{g},\sigma_{t,2}^{g'},\sigma_{t,3}^{g''}\right)$ Min. value = -2.94×10^{-4} at $g=g'=g''=16$	$\boldsymbol{S}^{(3)}\left(\sigma_{t,2}^{g},\sigma_{t,2}^{g'},\sigma_{t,4}^{g''}\right)$ Min. value = -1.92×10^{-4} at $g=g'=g''=16$	$\boldsymbol{S}^{(3)}\left(\sigma_{t,2}^{g},\sigma_{t,2}^{g'},\sigma_{t,5}^{g''}\right)$ Min. value = -3.66×10^{-2} at $g=g'=27, g''=30$	$\boldsymbol{S}^{(3)}\left(\sigma_{t,2}^{g},\sigma_{t,2}^{g'},\sigma_{t,6}^{g''}\right)$ Min. value = -4.37×10^{-1} at $g=g'=27, g''=30$
$k=3$ (^{69}Ga)		$\boldsymbol{S}^{(3)}\left(\sigma_{t,2}^{g},\sigma_{t,3}^{g'},\sigma_{t,3}^{g''}\right)$ Min. value = -1.54×10^{-5} at $g=g'=g''=16$	$\boldsymbol{S}^{(3)}\left(\sigma_{t,2}^{g},\sigma_{t,3}^{g'},\sigma_{t,4}^{g''}\right)$ Min. value = -1.01×10^{-5} at $g=g'=g''=16$	$\boldsymbol{S}^{(3)}\left(\sigma_{t,2}^{g},\sigma_{t,3}^{g'},\sigma_{t,5}^{g''}\right)$ Min. value = -1.50×10^{-3} at $g=g'=12, g''=30$	$\boldsymbol{S}^{(3)}\left(\sigma_{t,2}^{g},\sigma_{t,3}^{g'},\sigma_{t,6}^{g''}\right)$ Min. value = -1.78×10^{-2} at $g=g'=12, g''=30$
$k=4$ (^{71}Ga)			$\boldsymbol{S}^{(3)}\left(\sigma_{t,2}^{g},\sigma_{t,4}^{g'},\sigma_{t,4}^{g''}\right)$ Min. value = -2.94×10^{-5} at $g=g'=g''=22$	$\boldsymbol{S}^{(3)}\left(\sigma_{t,2}^{g},\sigma_{t,4}^{g'},\sigma_{t,5}^{g''}\right)$ Min. value = -1.01×10^{-3} at $g=g'=12, g''=30$	$\boldsymbol{S}^{(3)}\left(\sigma_{t,2}^{g},\sigma_{t,4}^{g'},\sigma_{t,6}^{g''}\right)$ Min. value = -1.21×10^{-2} at $g=g'=12, g''=30$
$k=5$ (C)				$\boldsymbol{S}^{(3)}\left(\sigma_{t,2}^{g},\sigma_{t,5}^{g'},\sigma_{t,5}^{g''}\right)$ 75 elements with absolute value > 1.0	$\boldsymbol{S}^{(3)}\left(\sigma_{t,2}^{g},\sigma_{t,5}^{g'},\sigma_{t,6}^{g''}\right)$ 452 elements with absolute values > 1.0
$k=6$ (^{1}H)					$\boldsymbol{S}^{(3)}\left(\sigma_{t,2}^{g},\sigma_{t,6}^{g'},\sigma_{t,6}^{g''}\right)$ 1621 elements with absolute values > 1.0

Table 11. Summary presentation of the distinct submatrices within the matrix $\boldsymbol{S}^{(3)}\left(\sigma_{t,j=3}^{g},\sigma_{t,k}^{g'},\sigma_{t,l}^{g''}\right), j=3; k,l=1,\cdots,6; g,g',g''=1,\cdots,30$.

Isotopes	$l=3$ (^{69}Ga)	$l=4$ (^{71}Ga)	$l=5$ (C)	$l=6$ (^{1}H)
$k=3$ (^{69}Ga)	$\boldsymbol{S}^{(3)}\left(\sigma_{t,3}^{g},\sigma_{t,3}^{g'},\sigma_{t,3}^{g''}\right)$ Min. value = -8.09×10^{-7} at $g=g'=g''=16$	$\boldsymbol{S}^{(3)}\left(\sigma_{t,3}^{g},\sigma_{t,3}^{g'},\sigma_{t,4}^{g''}\right)$ Min. value = -5.27×10^{-7} at $g=g'=g''=16$	$\boldsymbol{S}^{(3)}\left(\sigma_{t,3}^{g},\sigma_{t,3}^{g'},\sigma_{t,5}^{g''}\right)$ Min. value = -6.80×10^{-5} at $g=g'=13, g''=30$	$\boldsymbol{S}^{(3)}\left(\sigma_{t,3}^{g},\sigma_{t,3}^{g'},\sigma_{t,6}^{g''}\right)$ Min. value = -8.11×10^{-4} at $g=g'=13, g''=30$
$k=4$ (^{71}Ga)		$\boldsymbol{S}^{(3)}\left(\sigma_{t,3}^{g},\sigma_{t,4}^{g'},\sigma_{t,4}^{g''}\right)$ Min. value = -1.10×10^{-6} at $g=12, g'=g''=22$	$\boldsymbol{S}^{(3)}\left(\sigma_{t,3}^{g},\sigma_{t,4}^{g'},\sigma_{t,5}^{g''}\right)$ Min. value = -4.58×10^{-5} at $g=g'=13, g''=30$	$\boldsymbol{S}^{(3)}\left(\sigma_{t,3}^{g},\sigma_{t,4}^{g'},\sigma_{t,6}^{g''}\right)$ Min. value = -5.47×10^{-4} at $g=g'=13, g''=30$
$k=5$ (C)			$\boldsymbol{S}^{(3)}\left(\sigma_{t,3}^{g},\sigma_{t,5}^{g'},\sigma_{t,5}^{g''}\right)$ Min. value = -7.27×10^{-2} at $g=g'=g''=30$	$\boldsymbol{S}^{(3)}\left(\sigma_{t,3}^{g},\sigma_{t,5}^{g'},\sigma_{t,6}^{g''}\right)$ Min. value = -8.68×10^{-1} at $g=g'=g''=30$
$k=6$ (^{1}H)				$\boldsymbol{S}^{(3)}\left(\sigma_{t,3}^{g},\sigma_{t,6}^{g'},\sigma_{t,6}^{g''}\right)$ 15 elements with absolute values > 1.0

Table 12. Summary presentation of the distinct submatrices within the matrix $S^{(3)}\left(\sigma_{t,j=4}^{g},\sigma_{t,k}^{g'},\sigma_{t,l}^{g''}\right), j=4; k,l=1,\cdots,6; g,g',g''=1,\cdots,30$.

Isotopes	$l=4$ (^{71}Ga)	$l=5$ (C)	$l=6$ (^{1}H)
$k=4$ (^{71}Ga)	$S^{(3)}\left(\sigma_{t,4}^{g},\sigma_{t,4}^{g'},\sigma_{t,4}^{g''}\right)$ Min. value = -1.36×10^{-5} at $g=12, g'=g''=22$	$S^{(3)}\left(\sigma_{t,4}^{g},\sigma_{t,4}^{g'},\sigma_{t,5}^{g''}\right)$ Min. value = -2.11×10^{-4} at $g=g'=22, g''=30$	$S^{(3)}\left(\sigma_{t,4}^{g},\sigma_{t,4}^{g'},\sigma_{t,6}^{g''}\right)$ Min. value = -2.52×10^{-3} at $g=g'=22, g''=30$
$k=5$ (C)		$S^{(3)}\left(\sigma_{t,4}^{g},\sigma_{t,5}^{g'},\sigma_{t,5}^{g''}\right)$ Min. value = -4.76×10^{-2} at $g=g'=g''=30$	$S^{(3)}\left(\sigma_{t,4}^{g},\sigma_{t,5}^{g'},\sigma_{t,6}^{g''}\right)$ Min. value = -5.69×10^{-1} at $g=g'=g''=30$
$k=6$ (^{1}H)			$S^{(3)}\left(\sigma_{t,4}^{g},\sigma_{t,6}^{g'},\sigma_{t,6}^{g''}\right)$ 11 elements with absolute values > 1.0

Table 13. Summary presentation of the distinct submatrices within the matrix $S^{(3)}\left(\sigma_{t,j=5}^{g},\sigma_{t,k}^{g'},\sigma_{t,l}^{g''}\right), j=5; k,l=1,\cdots,6; g,g',g''=1,\cdots,30$.

Isotopes	$l=5$ (C)	$l=6$ (^{1}H)
$k=5$ (C)	$S^{(3)}\left(\sigma_{t,5}^{g},\sigma_{t,5}^{g'},\sigma_{t,5}^{g''}\right)$ 16 elements with absolute values > 1.0	$S^{(3)}\left(\sigma_{t,5}^{g},\sigma_{t,5}^{g'},\sigma_{t,6}^{g''}\right)$ 179 elements with absolute values > 1.0
$k=6$ (^{1}H)		$S^{(3)}\left(\sigma_{t,5}^{g},\sigma_{t,6}^{g'},\sigma_{t,6}^{g''}\right)$ 1563 elements with absolute values > 1.0

Table 14. Summary presentation of the distinct submatrices within the matrix $S^{(3)}\left(\sigma_{t,j=6}^{g},\sigma_{t,k}^{g'},\sigma_{t,l}^{g''}\right), j=6; k,l=1,\cdots,6; g,g',g''=1,\cdots,30$.

Isotopes	$l=6$ (^{1}H)
$k=6$ (^{1}H)	$S^{(3)}\left(\sigma_{t,6}^{g},\sigma_{t,6}^{g'},\sigma_{t,6}^{g''}\right)$ 6999 elements with absolute values > 1.0

The submatrices which comprise components having absolute values greater than 1.0, as shown in **Tables 9-14**, will be discussed in detail in sub-Sections 3.1-3.16, below.

3.1. Third-Order Relative Sensitivities $S^{(3)}\left(\sigma_{t,j=1}^{g},\sigma_{t,k=1}^{g'},\sigma_{t,l=1}^{g''}\right), g,g',g''=1,\cdots,30$

The values of the 3rd-order relative sensitivities of the leakage response with respect to the microscopic total cross sections for isotope 1 (^{239}Pu) are all nega-

tive. As summarized in Table 9, the $G\times G\times G=30\times 30\times 30$ dimensional submatrix $\boldsymbol{S}^{(3)}\left(\sigma_{t,j=1}^{g},\sigma_{t,k=1}^{g'},\sigma_{t,l=1}^{g''}\right),g,g',g''=1,\cdots,30$, comprises 2027 elements that have absolute values greater than 1.0. Figure 1 depicts the distribution of those 2027 large sensitivities in a three-dimensional (3D) plot, where the energy groups $g,g',g''=1,\cdots,30$ that characterize a parameter $\sigma_{t,j=1}^{g},\sigma_{t,k=1}^{g'},\sigma_{t,l=1}^{g''}$ appear on the 3D-plot's respective axes. The absolute values of these 2027 elements are illustrated by spheres, where the size and color of each sphere indicate visually the magnitude of the respective relative sensitivity. In addition, Figure 1 also shows the projection (colored in grey) of the 3rd-order mixed relative sensitivities onto the bottom plane, *i.e.*, the g–g′plane. As shown in Figure 1, most of these large sensitivities concentrate in the cubic region confined by the energy groups of $g,g',g''=6,\cdots,22$, and some appear on the surface defined by $g=30$, $g'=30$ and $g''=30$, respectively. Among the 2027 large elements plotted in Figure 1, the majority (1803 out of 2027) have absolute values in the range of 1.0 - 5.0; 206 elements have absolute values in the range of 5.0 - 10.0; only 18 elements have absolute values greater than 10.0. The largest (*i.e.*, the most negative) 3rd-order relative sensitivity in the submatrix $\boldsymbol{S}^{(3)}\left(\sigma_{t,j=1}^{g},\sigma_{t,k=1}^{g'},\sigma_{t,l=1}^{g''}\right),g,g',g''=1,\cdots,30$ is $S^{(3)}\left(\sigma_{t,1}^{g=12},\sigma_{t,1}^{g'=12},\sigma_{t,1}^{g''=12}\right)=-23.71$, which occurs for the 12th energy group of the total cross section for isotope 1 (^{239}Pu).

3.2. Third-Order Relative Sensitivities $\boldsymbol{S}^{(3)}\left(\sigma_{t,j=1}^{g},\sigma_{t,k=1}^{g'},\sigma_{t,l=2}^{g''}\right),g,g',g''=1,\cdots,30$

The values of the 3rd-order mixed relative sensitivities belonging to the submatrix $\boldsymbol{S}^{(3)}\left(\sigma_{t,j=1}^{g},\sigma_{t,k=1}^{g'},\sigma_{t,l=2}^{g''}\right),g,g',g''=1,\cdots,30$ are all negative. In this submatrix, only 4 elements have absolute values greater than 1.0, as listed in Table 15. Notably, all these 4 elements are located on the diagonal of this three-dimensional submatrix, with $g=g'=g''=12$, $g=g'=g''=13$, $g=g'=g''=14$, and $g=g'=g''=16$, respectively. The largest value among these sensitivities is attained by the 3rd-order mixed relative sensitivity $S^{(3)}\left(\sigma_{t,1}^{g=12},\sigma_{t,1}^{g'=12},\sigma_{t,2}^{g''=12}\right)=-1.50$ of the leakage response with respect to the total cross sections $\sigma_{t,1}^{g=12}$, $\sigma_{t,1}^{g'=12}$ and $\sigma_{t,2}^{g''=12}$, all in energy group 12.

Table 15. Components of $\boldsymbol{S}^{(3)}\left(\sigma_{t,j=1}^{g},\sigma_{t,k=1}^{g'},\sigma_{t,l=2}^{g''}\right),g,g',g''=1,\cdots,30$ having absolute values greater than 1.0.

Components	Values
$S^{(3)}\left(\sigma_{t,1}^{g=12},\sigma_{t,1}^{g'=12},\sigma_{t,2}^{g''=12}\right)$	−1.50
$S^{(3)}\left(\sigma_{t,1}^{g=13},\sigma_{t,1}^{g'=13},\sigma_{t,2}^{g''=13}\right)$	−1.30
$S^{(3)}\left(\sigma_{t,1}^{g=14},\sigma_{t,1}^{g'=14},\sigma_{t,2}^{g''=14}\right)$	−1.14
$S^{(3)}\left(\sigma_{t,1}^{g=16},\sigma_{t,1}^{g'=16},\sigma_{t,2}^{g''=16}\right)$	−1.44

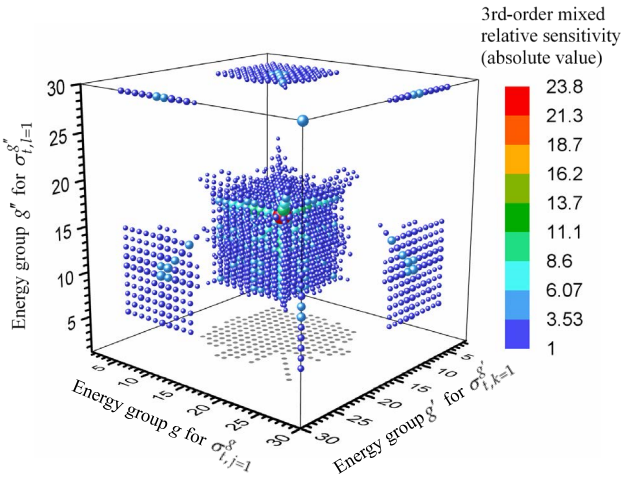

Figure 1. The matrix of sensitivities $\boldsymbol{S}^{(3)}\left(\sigma^{g}_{t,\,j=1},\sigma^{g'}_{t,\,k=1},\sigma^{g''}_{t,\,l=1}\right),\ g,g',g''=1,\cdots,30$ for ^{239}Pu; only elements having absolute values greater than 1.0 are depicted.

3.3. Third-Order Relative Sensitivities $\boldsymbol{S}^{(3)}\left(\sigma^{g}_{t,\,j=1},\sigma^{g'}_{t,\,k=1},\sigma^{g''}_{t,\,l=5}\right),\ g,g',g''=1,\cdots,30$

The submatrix $\boldsymbol{S}^{(3)}\left(\sigma^{g}_{t,\,j=1},\sigma^{g'}_{t,\,k=1},\sigma^{g''}_{t,\,l=5}\right),\ g,g',g''=1,\cdots,30$ comprises the 3rd-order mixed relative sensitivities of the leakage response with respect to the total cross sections of isotope 1 (^{239}Pu) and isotope 5 (C). Among the total 27,000 components in the submatrix, the majority of them (namely, 25,259 components) have negative sensitivities, with values between −8.3 and 0; only few components (e.g., 1741 components) have positive sensitivities, which are very small having values in the order of 10^{-4} or less. The submatrix $\boldsymbol{S}^{(3)}\left(\sigma^{g}_{t,\,j=1},\sigma^{g'}_{t,\,k=1},\sigma^{g''}_{t,\,l=5}\right),\ g,g',g''=1,\cdots,30$ comprises only 188 components that have absolute values greater than 1.0; these components are depicted in **Figure 2**. As shown in this figure, 38 components having absolute values between 1.0 and 2.0 are located inside the region confined by the energy groups of $g,g'=12,\cdots,16$ and $g''=12,\cdots,22$; the remaining 150 elements are located on the surface defined by $g''=30$, and have absolute values in the range from 1.0 to 8.3. Of these 150 elements (on the surface $g''=30$), 23 elements are located on the edges, and the others are concentrated in the square region defined by the energy groups $g,g'=7,\cdots,17$. The most negative 3rd-order relative sensitivity in the submatrix $\boldsymbol{S}^{(3)}\left(\sigma^{g}_{t,\,j=1},\sigma^{g'}_{t,\,k=1},\sigma^{g''}_{t,\,l=5}\right),\ g,g',g''=1,\cdots,30$ is $S^{(3)}\left(\sigma^{g=12}_{t,1},\sigma^{g'=12}_{t,1},\sigma^{g''=30}_{t,5}\right)=-8.29$, which involves the 12th energy group of the total cross section for isotope 1 (^{239}Pu) and the 30th energy group of the total cross section for isotope 5 (C).

3.4. Third-Order Relative Sensitivities $\boldsymbol{S}^{(3)}\left(\sigma^{g}_{t,\,j=1},\sigma^{g'}_{t,\,k=1},\sigma^{g''}_{t,\,l=6}\right),\ g,g',g''=1,\cdots,30$

The submatrix $\boldsymbol{S}^{(3)}\left(\sigma^{g}_{t,\,j=1},\sigma^{g'}_{t,\,k=1},\sigma^{g''}_{t,\,l=6}\right),\ g,g',g''=1,\cdots,30$ comprises the

3rd-order mixed relative sensitivities of the leakage response with respect to the microscopic total cross sections of isotope 1 (^{239}Pu) and isotope 6 (^{1}H). The majority (*i.e.*, 25,259 out of the total 27,000) of the components of this submatrix have negative values. The remaining 1741 components have positive values, which are very small (of the order of 10^{-3} and smaller). The matrix $\boldsymbol{S}^{(3)}\left(\sigma_{t,\,j=1}^{g},\sigma_{t,\,k=1}^{g'},\sigma_{t,\,l=6}^{g''}\right), g,g',g''=1,\cdots,30$ includes 3090 components that have absolute values greater than 1.0. These 3090 components are depicted in Figure 3, which indicates that: 1) 2923 components (ca. 95% of 3090) have absolute values in the range between 1.0 and 10.0, located mostly inside the region confined by the energy groups of $g,g'=5,\cdots,27$, and $g''=7,\cdots,30$; 2) 155 components

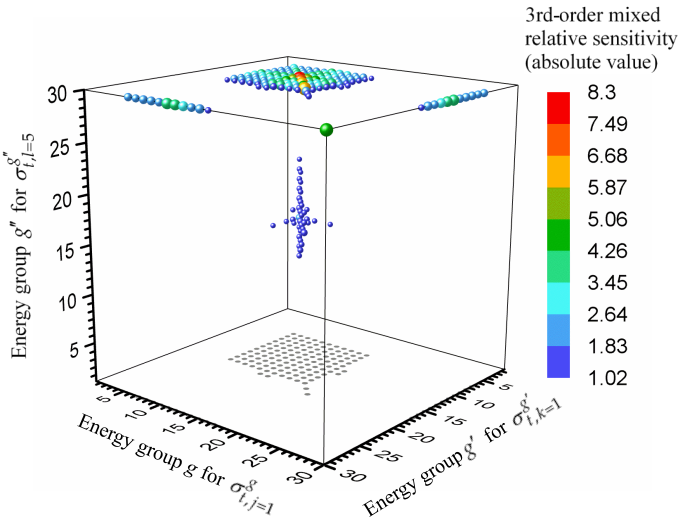

Figure 2. The matrix of sensitivities $\boldsymbol{S}^{(3)}\left(\sigma_{t,\,j=1}^{g},\sigma_{t,\,k=1}^{g'},\sigma_{t,\,l=5}^{g''}\right), g,g',g''=1,\cdots,30$; only elements having absolute values greater than 1.0 are depicted.

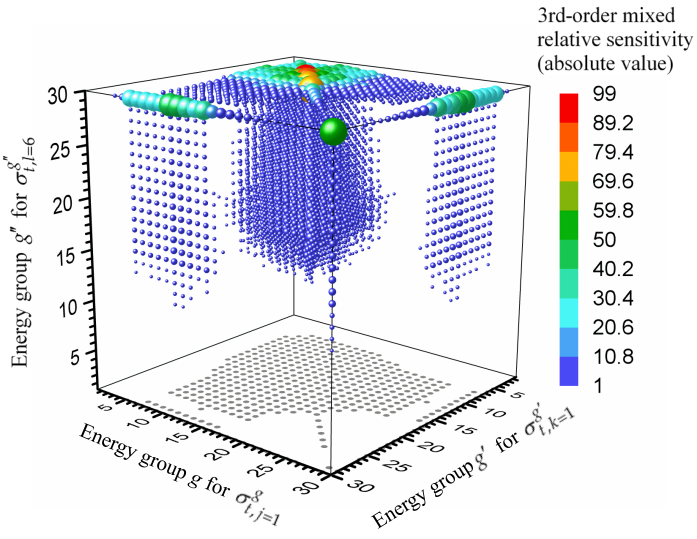

Figure 3. The matrix of sensitivities $\boldsymbol{S}^{(3)}\left(\sigma_{t,\,j=1}^{g},\sigma_{t,\,k=1}^{g'},\sigma_{t,\,l=6}^{g''}\right), g,g',g''=1,\cdots,30$; only elements having absolute values greater than 1.0 are depicted.

(ca. 5% of 3090) have absolute values between 10.0 and 50.0; and 3) 12 components have absolute values between 50.0 and 99.0. As illustrated in Figure 3, the components of $\boldsymbol{S}^{(3)}\left(\sigma_{t,\,j=1}^{g},\sigma_{t,\,k=1}^{g'},\sigma_{t,\,l=6}^{g''}\right), g,g',g''=1,\cdots,30$ having absolute values greater than 10.0 are mostly located on the surface defined by $g''=30$. In the submatrix $\boldsymbol{S}^{(3)}\left(\sigma_{t,\,j=1}^{g},\sigma_{t,\,k=1}^{g'},\sigma_{t,\,l=6}^{g''}\right), g,g',g''=1,\cdots,30$, the most negative 3rd-order mixed relative sensitivity is $S^{(3)}\left(\sigma_{t,1}^{g=12},\sigma_{t,1}^{g'=12},\sigma_{t,6}^{g''=30}\right)=-98.98$, which involves the 12th energy group of the total cross section for isotope 1 (^{239}Pu) and the 30th energy group of the total cross section for isotope 6 (^{1}H).

3.5. Third-Order Relative Sensitivities $S^{(3)}\left(\sigma_{t,j=1}^{g},\sigma_{t,k=2}^{g'},\sigma_{t,l=6}^{g''}\right), g,g',g''=1,\cdots,30$

The submatrix $\boldsymbol{S}^{(3)}\left(\sigma_{t,\,j=1}^{g},\sigma_{t,\,k=2}^{g'},\sigma_{t,\,l=6}^{g''}\right), g,g',g''=1,\cdots,30$ comprises the 3rd-order mixed relative sensitivities of the leakage response with respect to the microscopic total cross sections of isotope 1 (^{239}Pu), isotope 2 (^{240}Pu) and isotope 6 (^{1}H). As was the case for the submatrices investigated in the foregoing (cf. sections 3.3 and 3.4), 25,259 of the 27,000 components in the submatrix have negative values; the remaining 1741 components have very small positive values, of the order of 10^{-4} or less. Figure 4 depicts the 120 components of this submatrix which have absolute values greater than 1.0. As shown in the figure, all these 120 components are located on the surface defined by $g''=30$, concentrated in the square region delimited by energy groups $g,g'=7,\cdots,17$. The most negative 3rd-order relative sensitivity in the submatrix is $S^{(3)}\left(\sigma_{t,1}^{g=12},\sigma_{t,2}^{g'=12},\sigma_{t,6}^{g''=30}\right)=-6.27$, which involves the 12th energy group of the total cross section for ^{239}Pu, ^{240}Pu and the 30th energy group of the total cross section for ^{1}H.

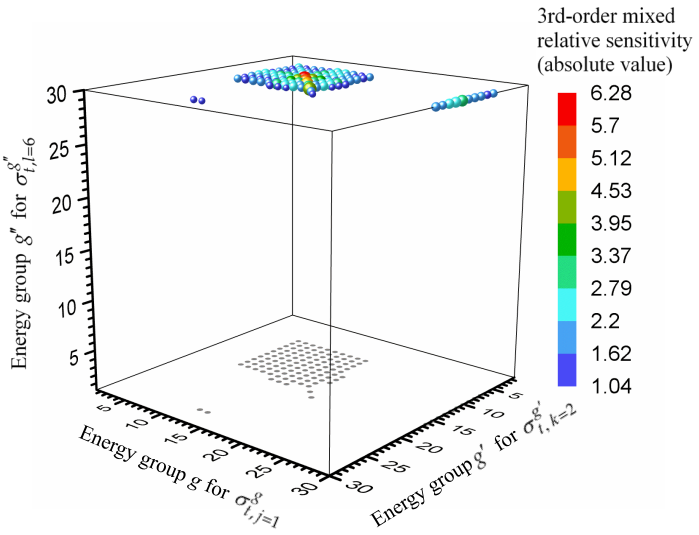

Figure 4. The matrix of sensitivities $\boldsymbol{S}^{(3)}\left(\sigma_{t,\,j=1}^{g},\sigma_{t,\,k=2}^{g'},\sigma_{t,\,l=6}^{g''}\right), g,g',g''=1,\cdots,30$; only elements having absolute values greater than 1.0 are depicted.

3.6. Third-Order Relative Sensitivities $S^{(3)}\left(\sigma_{t,j=1}^{g},\sigma_{t,k=5}^{g'},\sigma_{t,l=5}^{g''}\right), g,g',g''=1,\cdots,30$

The submatrix $\boldsymbol{S}^{(3)}\left(\sigma_{t,\,j=1}^{g},\sigma_{t,\,k=5}^{g'},\sigma_{t,\,l=5}^{g''}\right), g,g',g''=1,\cdots,30$ comprises the 3rd-order mixed relative sensitivities of the leakage response with respect to the microscopic total cross sections of isotopes ^{239}Pu, C and C. In this submatrix, 23,881 (out of the total 27,000) components have negative values, while the remaining 3119 components have positive values. All the positive values are very small (of the order of 10^{-4} or less) whereas the negative values are widely spread between 0.0 and −1319.5. Among the negative components, 817 components have 3rd-order mixed relative sensitivities with absolute values greater than 1.0. The magnitudes and distribution of these 817 components are illustrated in Figure 5. Due to the wide spread of the values of these components, Figure 5 employs a logarithm scale (instead of the linear scale employed in Figures 1-4) for scaling the size of the spheres as well as for the legend of the colors. As shown in Figure 5, most of the large sensitivities are concentrated in the region confined by energy groups $g=25,28,29,30$, $g'=7,\cdots,30$, and $g''=7,\cdots,30$. Among these 817 large sensitivities, 729 of them (*i.e.*, around 90%) have absolute values between 1.0 and 10.0, and 79 of them (*i.e.*, around 9%) are in the range of 10.0 to 100.0. The largest 9 sensitivities have values larger than 100.0 and are all located on the two edges of the surface defined by $g=30$, the largest of them being $S^{(3)}\left(\sigma_{t,1}^{g=30},\sigma_{t,5}^{g'=30},\sigma_{t,5}^{g''=30}\right)=-1319.5$, which involves the 30th energy group of the microscopic total cross section for isotope 1 (^{239}Pu), isotope 5 (C) and isotope 5 (C).

3.7. Third-Order Relative Sensitivities $S^{(3)}\left(\sigma_{t,j=1}^{g},\sigma_{t,k=6}^{g'},\sigma_{t,l=6}^{g''}\right), g,g',g''=1,\cdots,30$

The submatrix $\boldsymbol{S}^{(3)}\left(\sigma_{t,\,j=1}^{g},\sigma_{t,\,k=6}^{g'},\sigma_{t,\,l=6}^{g''}\right), g,g',g''=1,\cdots,30$ comprises the 3rd-order mixed relative sensitivities of the leakage response with respect to the microscopic total cross sections of isotope 1 (^{239}Pu), isotope 6 (^{1}H) and isotope 6 (^{1}H). As in the cases analyzed in the foregoing, most (namely: 23,881 out of 27,000) components of this submatrix have negative values spread in the wide range from 0.0 to -1.9×10^{5}. Only a relatively small number (namely 3119 components out of 27,000) have positive values; these positive values are very small, of the order of 10^{-3} or less. The submatrix $\boldsymbol{S}^{(3)}\left(\sigma_{t,\,j=1}^{g},\sigma_{t,\,k=6}^{g'},\sigma_{t,\,l=6}^{g''}\right), g,g',g''=1,\cdots,30$, comprises 7998 components which have absolute values greater than 1.0, which are depicted in Figure 6. Among the 7998 components, 6243 (ca. 78%) have absolute values between 1.0 and 10.0; 1266 components (ca. 16%) have absolute values between 10.0 and 100.0; 420 components (ca. 5%) have absolute values between 100.0 and 1000.0; and 69 components (ca. 1%) have absolute values between 1000.0 and 1.9×10^{5}. Due to the very wide range of values, these 3rd-order relative sensitivities are plotted on a log scale in Figure 6. The components having absolute values greater than

1000.0 are mostly located on the surface defined by $g=30$. In the submatrix $\mathbf{S}^{(3)}\left(\sigma_{t,\,j=1}^{g},\sigma_{t,\,k=6}^{g'},\sigma_{t,\,l=6}^{g''}\right),\ g,g',g''=1,\cdots,30$, the largest 3rd-order mixed relative sensitivity is $S^{(3)}\left(\sigma_{t,1}^{g=30},\sigma_{t,6}^{g'=30},\sigma_{t,6}^{g''=30}\right)=-1.88\times10^{5}$, which involves the 30th energy groups of the total cross section for isotope 1 (^{239}Pu), isotope 6 (^{1}H) and isotope 6 (^{1}H).

3.8. Third-Order Relative Sensitivities $S^{(3)}\left(\sigma_{t,j=2}^{g},\sigma_{t,k=5}^{g'},\sigma_{t,l=5}^{g''}\right),\ g,g',g''=1,\cdots,30$

The submatrix $\mathbf{S}^{(3)}\left(\sigma_{t,\,j=2}^{g},\sigma_{t,\,k=5}^{g'},\sigma_{t,\,l=5}^{g''}\right),\ g,g',g''=1,\cdots,30$ comprises the 3rd-order mixed relative sensitivities of the leakage response with respect to the microscopic total cross sections of isotopes ^{240}Pu, C and C. As was the case for

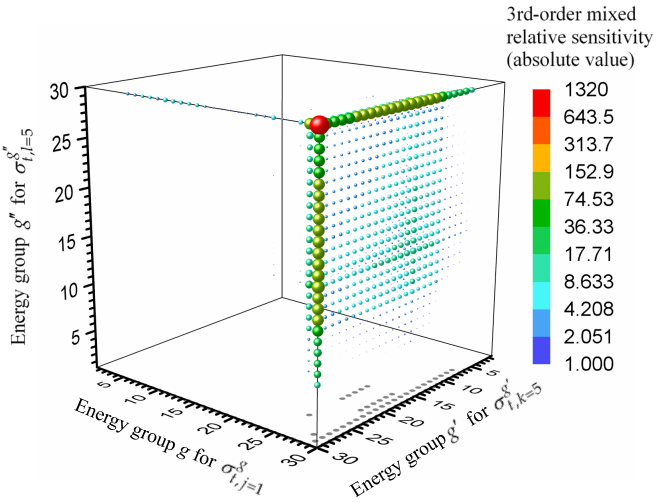

Figure 5. The matrix of sensitivities $\mathbf{S}^{(3)}\left(\sigma_{t,\,j=1}^{g},\sigma_{t,\,k=5}^{g'},\sigma_{t,\,l=5}^{g''}\right),\ g,g',g''=1,\cdots,30$; only elements having absolute values greater than 1.0 are depicted.

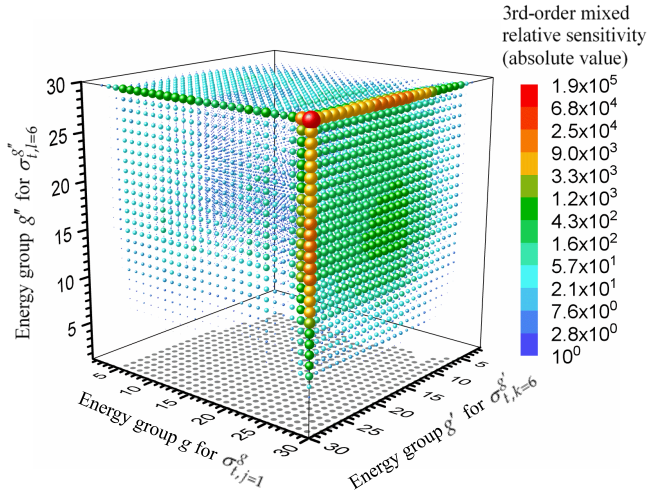

Figure 6. The matrix of sensitivities $\mathbf{S}^{(3)}\left(\sigma_{t,\,j=1}^{g},\sigma_{t,\,k=6}^{g'},\sigma_{t,\,l=6}^{g''}\right),\ g,g',g''=1,\cdots,30$; only elements having absolute values greater than 1.0 are depicted.

the submatrices discussed in the foregoing, the values of the 3rd-order mixed relative sensitivities for the majority (namely, 23,881 out of 27,000) of the components of this submatrix are negative, having values from 0.0 to −22.7, whereas the other 3119 components have very small positive values (of the order of 10^{-5} or less). Figure 7 displays the magnitudes and distribution of the 75 components of this submatrix which have absolute values greater than 1.0. As shown in this figure, most of these 75 large sensitivities are located in the region delimited by energy groups $g=28,30$, $g'=12,\cdots,30$ and $g''=12,\cdots,30$. Among the 75 large sensitivities, 73 of them have absolute values between 1.0 and 5.0. Only 2 components have absolute values larger than 5.0, namely: $S^{(3)}\left(\sigma_{t,2}^{g=28},\sigma_{t,5}^{g'=30},\sigma_{t,5}^{g''=30}\right)=-17.09$, and $S^{(3)}\left(\sigma_{t,2}^{g=30},\sigma_{t,5}^{g'=30},\sigma_{t,5}^{g''=30}\right)=-22.63$; the largest component involves the 30th energy group of the microscopic total cross sections for isotopes ^{240}Pu, C and C, respectively.

3.9. Third-Order Relative Sensitivities $S^{(3)}\left(\sigma_{t,j=2}^{g},\sigma_{t,k=5}^{g'},\sigma_{t,l=6}^{g''}\right),\ g,g',g''=1,\cdots,30$

The submatrix $S^{(3)}\left(\sigma_{t,\ j=2}^{g},\sigma_{t,\ k=5}^{g'},\sigma_{t,\ l=6}^{g''}\right),\ g,g',g''=1,\cdots,30$ comprises the 3rd-order mixed relative sensitivities of the leakage response with respect to the microscopic total cross sections of isotopes ^{240}Pu, C and ^{1}H. Similarly, among the 27,000 components in this submatrix, the majority (namely: 23,881 of 27,000) of these components have negative values for the 3rd-order mixed relative sensitivities, having values in the range from 0.0 to −271.0; the other 3119 components have very small positive values (of the order of 10^{-4} or less). Figure 8 shows the magnitudes and distribution of the 452 third-order relative sensitivities having absolute values greater than 1.0. As shown in this figure, most of these large sensitivities are located in the region delimited by energy groups $g=27,28,30$, $g'=12,\cdots,30$ and $g''=12,\cdots,30$. Among these 452 components, 370 of them

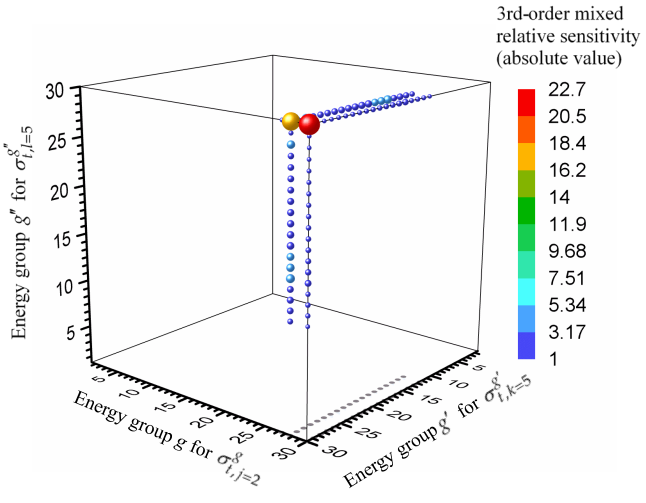

Figure 7. The matrix of sensitivities $S^{(3)}\left(\sigma_{t,\ j=2}^{g},\sigma_{t,\ k=5}^{g'},\sigma_{t,\ l=5}^{g''}\right),\ g,g',g''=1,\cdots,30$; only elements having absolute values greater than 1.0 are depicted.

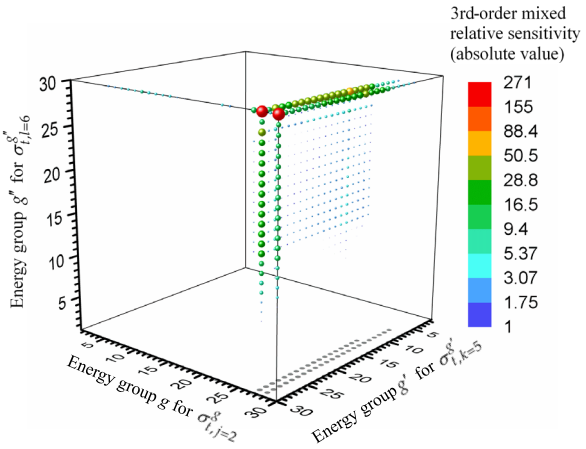

Figure 8. The matrix of sensitivities $\boldsymbol{S}^{(3)}\left(\sigma_{t,\,j=2}^{g},\sigma_{t,\,k=5}^{g'},\sigma_{t,\,l=6}^{g''}\right), g,g',g''=1,\cdots,30$; only elements having absolute values greater than 1.0 are depicted.

(ca. 82%) have absolute values between 1.0 and 5.0; 16 components have values in the range 5.0 to 10.0; and 63 components have values between 10.0 and 50.0; only 3 components have absolute values larger than 50.0. The largest 3rd-order mixed relative sensitivities in this submatrix is $S^{(3)}\left(\sigma_{t,2}^{g=30},\sigma_{t,5}^{g'=30},\sigma_{t,6}^{g''=30}\right)=-270.08$, which involves the 30th energy group of the microscopic total cross section for isotopes ^{240}Pu, C and ^{1}H.

3.10. Third-Order Relative Sensitivities $\boldsymbol{S}^{(3)}\left(\sigma_{t,\,j=2}^{g},\sigma_{t,k=6}^{g'},\sigma_{t,l=6}^{g''}\right), g,g',g''=1,\cdots,30$

The submatrix $\boldsymbol{S}^{(3)}\left(\sigma_{t,\,j=2}^{g},\sigma_{t,\,k=6}^{g'},\sigma_{t,\,l=6}^{g''}\right), g,g',g''=1,\cdots,30$, comprises the 3rd-order mixed relative sensitivities of the leakage response with respect to the microscopic total cross sections of isotopes ^{240}Pu, ^{1}H and ^{1}H. As was the case with the submatrices analyzed in the foregoing, 23,881 elements of this submatrix have negative values and only 3119 components have positives values; the positive values are very small (order of 10^{-4} or less) whereas the negative values range from 0.0 to -3.2×10^{3}. Using a logarithmic scale, **Figure 9** shows the distribution of the 1621 components of this submatrix which have absolute values greater than 1.0. Among these 1621 components, 1282 (ca. 79%) have absolute values between 1.0 to 10.0; 274 components (ca. 17%) have absolute values between 10.0 to 100.0; 63 components (ca. 4%) have absolute values between 100.0 to 1000.0; and 2 components have absolute values greater than 1000.0. As illustrated in the figure, those components with absolute values greater than 100.0 are mostly located on the planes defined by $g=28$ and $g=30$. The largest 3rd-order mixed relative sensitivity in the submatrix $\boldsymbol{S}^{(3)}\left(\sigma_{t,\,j=2}^{g},\sigma_{t,\,k=6}^{g'},\sigma_{t,\,l=6}^{g''}\right), g,g',g''=1,\cdots,30$, is $S^{(3)}\left(\sigma_{t,2}^{g=30},\sigma_{t,6}^{g'=30},\sigma_{t,6}^{g''=30}\right)=-3.22\times10^{3}$, which involves the 30th energy group of the total cross section for isotope 2 (^{240}Pu), isotope 6 (^{1}H) and isotope 6 (^{1}H). The next largest 3rd-order mixed relative sensitivity is $S^{(3)}\left(\sigma_{t,2}^{g=28},\sigma_{t,6}^{g'=30},\sigma_{t,6}^{g''=30}\right)=-2.43\times10^{3}$.

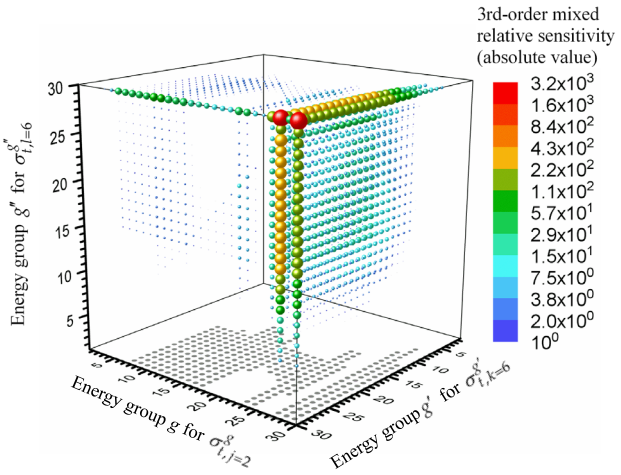

Figure 9. The matrix of sensitivities $S^{(3)}\left(\sigma^{g}_{t,\,j=2},\sigma^{g'}_{t,\,k=6},\sigma^{g''}_{t,\,l=6}\right),\ g,g',g''=1,\cdots,30$; only elements having absolute values greater than 1.0 are depicted.

3.11. Third-Order Relative Sensitivities $S^{(3)}\left(\sigma^{g}_{t,\,j=3},\sigma^{g'}_{t,k=6},\sigma^{g''}_{t,l=6}\right),\ g,g',g''=1,\cdots,30$

The submatrix $S^{(3)}\left(\sigma^{g}_{t,\,j=3},\sigma^{g'}_{t,\,k=6},\sigma^{g''}_{t,\,l=6}\right),\ g,g',g''=1,\cdots,30$ comprises the 3rd-order mixed relative sensitivities of the leakage response with respect to the microscopic total cross sections of isotopes ^{69}Ga, ^{1}H and ^{1}H. Likewise, among the 27,000 components in this submatrix, 23,881 components have negative values varying between −10.4 to 0.0; the rest 3119 components have very small positive values (of the order of 10^{-5} or less). Figure 10 shows the magnitudes and distribution of the 15 components of this submatrix which have absolute values greater than 1.0. As shown in this figure, these 15 components are located in the region delineated by $g'=g''=30$ and $g=7,\cdots,20,30$. The largest 3rd-order mixed relative sensitivity is $S^{(3)}\left(\sigma^{g=30}_{t,3},\sigma^{g'=30}_{t,6},\sigma^{g''=30}_{t,6}\right)=-10.36$, which involves the 30th energy group of the total cross section for isotope 3 (^{69}Ga), isotope 6 (^{1}H) and isotope 6 (^{1}H).

3.12. Third-Order Relative Sensitivities $S^{(3)}\left(\sigma^{g}_{t,\,j=4},\sigma^{g'}_{t,k=6},\sigma^{g''}_{t,l=6}\right),\ g,g',g''=1,\cdots,30$

The submatrix $S^{(3)}\left(\sigma^{g}_{t,\,j=4},\sigma^{g'}_{t,\,k=6},\sigma^{g''}_{t,\,l=6}\right),\ g,g',g''=1,\cdots,30$ comprises the 3rd-order mixed relative sensitivities of the leakage response with respect to the microscopic total cross sections of isotopes ^{71}Ga, ^{1}H and ^{1}H. Of the 27,000 components of this submatrix, 23,881 have negative values varying between 0.0 and −6.79; the remaining 3119 components have very small positive values (of the order of 10^{-5} or less). Figure 11 illustrates the distribution of the 11 components of $S^{(3)}\left(\sigma^{g}_{t,\,j=4},\sigma^{g'}_{t,\,k=6},\sigma^{g''}_{t,\,l=6}\right),\ g,g',g''=1,\cdots,30$ that have absolute values greater than 1.0. As shown in this figure, all of these 11 components are located on the surfaces defined by $g'=30$ and $g''=30$. The largest 3rd-order mixed relative sensitivity is $S^{(3)}\left(\sigma^{g=30}_{t,4},\sigma^{g'=30}_{t,6},\sigma^{g''=30}_{t,6}\right)=-6.79$, which involves the 30th

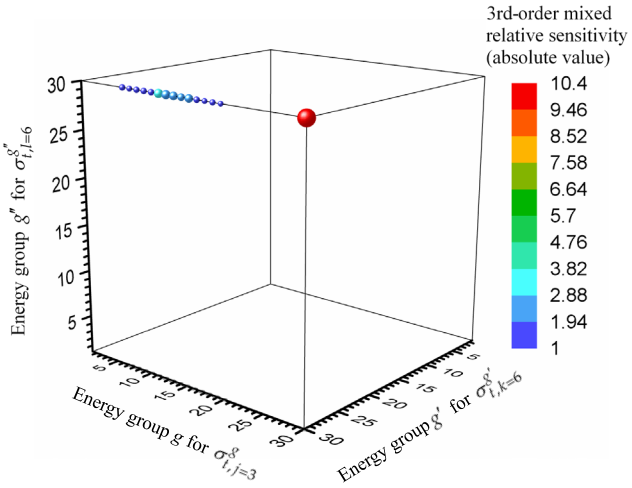

Figure 10. The matrix of sensitivities $S^{(3)}\left(\sigma_{t,\,j=3}^{g},\sigma_{t,\,k=6}^{g'},\sigma_{t,\,l=6}^{g''}\right),\ g,g',g''=1,\cdots,30$; only elements having absolute values greater than 1.0 are depicted.

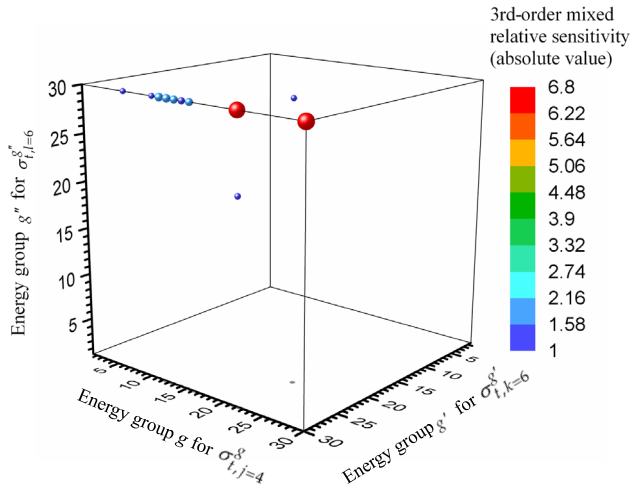

Figure 11. The matrix of sensitivities $S^{(3)}\left(\sigma_{t,\,j=4}^{g},\sigma_{t,\,k=6}^{g'},\sigma_{t,\,l=6}^{g''}\right),\ g,g',g''=1,\cdots,30$; only elements having absolute values greater than 1.0 are depicted.

energy group of the total cross section for isotope 4 (^{71}Ga), isotope 6 (^{1}H) and isotope 6 (^{1}H). The second largest 3rd-order mixed relative sensitivity is $S^{(3)}\left(\sigma_{t,4}^{g=22},\sigma_{t,6}^{g'=30},\sigma_{t,6}^{g''=30}\right)=-6.63$.

3.13. Third-Order Relative Sensitivities $S^{(3)}\left(\sigma_{t,\,j=5}^{g},\sigma_{t,k=5}^{g'},\sigma_{t,l=5}^{g''}\right),\ g,g',g''=1,\cdots,30$

The submatrix $S^{(3)}\left(\sigma_{t,\,j=5}^{g},\sigma_{t,\,k=5}^{g'},\sigma_{t,\,l=5}^{g''}\right),\ g,g',g''=1,\cdots,30$ comprises the 3rd-order mixed relative sensitivities of the leakage response with respect to the microscopic total cross sections of isotope C. This submatrix is symmetric about the principal diagonal defined by $g=g'=g''=0$ and $g=g'=g''=30$. The majority (*i.e.*, 23,207 out of 27,000) of this submatrix's components have negative values (varying between −17.45 and 0.0) while the remaining 3793 compo-

nents have very small positive values (of the order of 10^{-5} or less). Figure 12 shows the distribution of the 16 components of this submatrix which have absolute values greater than 1.0. As shown in the figure, all of these 16 components are located on the three edges of the cube. The largest 3rd-order mixed relative sensitivity is attained by $S^{(3)}\left(\sigma_{t,5}^{g=30},\sigma_{t,5}^{g'=30},\sigma_{t,5}^{g''=30}\right)=-17.45$, which occurs at the vertex of the cube, corresponding to the 30th energy group of the microscopic total cross section for isotope C.

3.14. Third-Order Relative Sensitivities $S^{(3)}\left(\sigma_{t,j=5}^{g},\sigma_{t,k=5}^{g'},\sigma_{t,l=6}^{g''}\right), g,g',g''=1,\cdots,30$

The submatrix $S^{(3)}\left(\sigma_{t,\,j=5}^{g},\sigma_{t,\,k=5}^{g'},\sigma_{t,\,l=6}^{g''}\right), g,g',g''=1,\cdots,30$ comprises the 3rd-order mixed relative sensitivities of the leakage response with respect to the microscopic total cross sections of isotopes C, C and ^{1}H. For this submatrix, 23,207 out of the 27,000 components have negative values, and the other 3739 components have positive values. The positive values are negligibly small (of the order of 10^{-4} or less) whereas the negative values vary from −208.2 to 0.0. Among the 23,207 negative values, 179 of them have absolute values greater than 1.0, and are depicted in Figure 13. As shown in this figure, 178 out of the 179 large sensitivities have absolute values ranging from 1.0 to 20.0. Only one component has an absolute value larger than 20.0, namely $S^{(3)}\left(\sigma_{t,5}^{g=30},\sigma_{t,5}^{g'=30},\sigma_{t,6}^{g''=30}\right)=-208.23$, which also involves the 30th energy group of the total cross section for isotopes C, C and ^{1}H.

3.15. Third-Order Relative Sensitivities $S^{(3)}\left(\sigma_{t,j=5}^{g},\sigma_{t,k=6}^{g'},\sigma_{t,l=6}^{g''}\right), g,g',g''=1,\cdots,30$

The submatrix $S^{(3)}\left(\sigma_{t,\,j=5}^{g},\sigma_{t,\,k=6}^{g'},\sigma_{t,\,l=6}^{g''}\right), g,g',g''=1,\cdots,30$ comprises the 3rd-order mixed relative sensitivities of the leakage response with respect to the

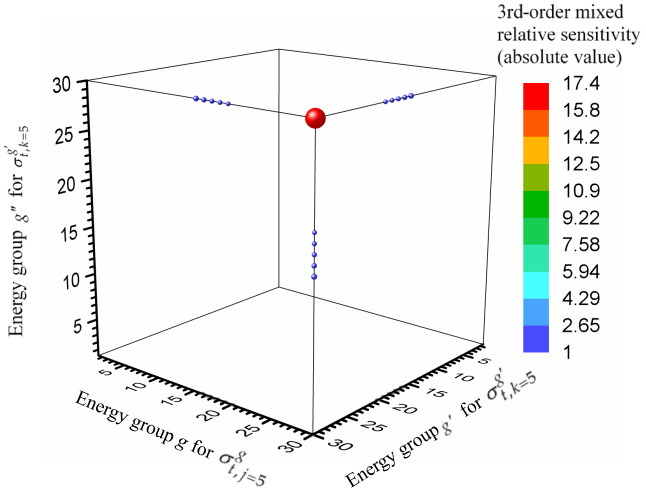

Figure 12. The matrix of sensitivities $S^{(3)}\left(\sigma_{t,\,j=5}^{g},\sigma_{t,\,k=5}^{g'},\sigma_{t,\,l=5}^{g''}\right), g,g',g''=1,\cdots,30$; only elements having absolute values greater than 1.0 are depicted.

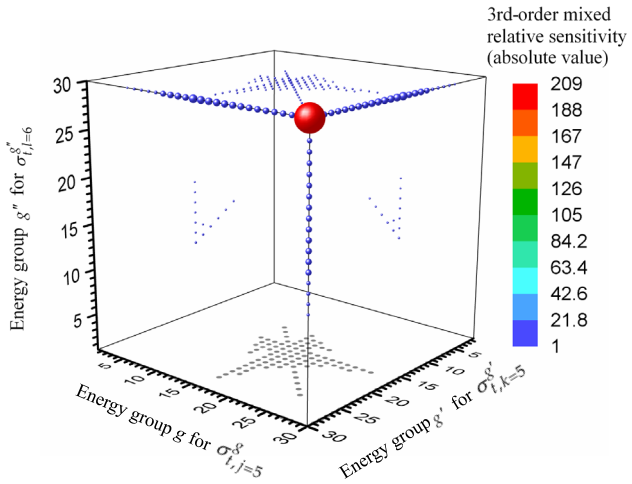

Figure 13. The matrix of sensitivities $\boldsymbol{S}^{(3)}\left(\sigma^{g}_{t,\,j=5},\sigma^{g'}_{t,\,k=5},\sigma^{g''}_{t,\,l=6}\right),\ g,g',g''=1,\cdots,30$; only elements having absolute values greater than 1.0 are depicted.

microscopic total cross sections of isotopes C, ^{1}H and ^{1}H. The majority (*i.e.*, 23,207 out of 27,000) of the components of this submatrix have negative values; the remaining 3793 components have positives values. Again, the positive values are very small, of the order of 10^{-4} or less; whereas the negative values span a wide range between -2.5×10^{3} and 0.0. Among the negative sensitivities, 1563 components have absolute values larger than 1.0, as illustrated in **Figure 14**. In this figure, a logarithmic scale is used to illustrate the magnitudes and the coloring of the absolute values, which are as follows: 1442 (ca. 92%) of the 1563 components have absolute values between 1.0 and 10.0; 92 components (ca. 6%) have absolute values between 10.0 and 100.0; 27 components (ca. 2%) have absolute values between 100.0 and 200.0; 2 components have absolute values greater than 200.0. As illustrated in **Figure 14**, most of the large components are located in the region confined by $g,g',g''=12,\cdots,30$; in particular, most of the components that have absolute values greater than 100.0 are located on the three edges of the cube. The largest 3rd-order mixed relative sensitivity in this submatrix is attained by $S^{(3)}\left(\sigma^{g=30}_{t,5},\sigma^{g'=30}_{t,6},\sigma^{g''=30}_{t,6}\right)=-2.49\times10^{3}$, involving the 30th energy group of the total cross section for isotopes C, ^{1}H and ^{1}H. The next largest 3rd-order mixed relative sensitivity is $S^{(3)}\left(\sigma^{g=16}_{t,5},\sigma^{g'=30}_{t,6},\sigma^{g''=30}_{t,6}\right)=-2.21\times10^{2}$.

3.16. Third-Order Relative Sensitivities $\boldsymbol{S}^{(3)}\left(\sigma^{g}_{t,\,j=6},\sigma^{g'}_{t,k=6},\sigma^{g''}_{t,l=6}\right),\ g,g',g''=1,\cdots,30$

Lastly, the submatrix $\boldsymbol{S}^{(3)}\left(\sigma^{g}_{t,\,j=6},\sigma^{g'}_{t,\,k=6},\sigma^{g''}_{t,\,l=6}\right),\ g,g',g''=1,\cdots,30$ comprises the 3rd-order mixed relative sensitivities of the leakage response with respect to the microscopic total cross sections of isotope 6 (^{1}H). Among the 27,000 components in this submatrix, 23,207 of them have negative values for the 3rd-order mixed relative sensitivities, which vary in the wide range from -2.97×10^{4} to 0.0; the other 3793 components have negligibly small positive values, of the order of 10^{-4} or less. There are 6999 components having absolute values greater than 1.0.

Figure 15 shows the distribution of these components on a logarithmic scale. Of these 6999 components, 5828 components (ca. 83.3%) have absolute values between 1.0 and 10.0; 1092 components (ca. 15.6%) have absolute values between 10.0 and 100.0; 51 components (ca. 0.7%) have absolute values between 100.0 and 1000.0; 27 components (ca. 0.4%) have absolute values between 1000.0 and 1500.0; and 1 component has absolute value greater than 1500.0. This largest component is the 3rd-order mixed relative sensitivity $S^{(3)}\left(\sigma_{t,6}^{g=30},\sigma_{t,6}^{g'=30},\sigma_{t,6}^{g''=30}\right)=-2.97\times10^{4}$, which involves the 30th energy group of the microscopic total cross section for isotope ^{1}H. As illustrated in Figure 15, most of these large components (having absolute values greater than 1.0) are located in the region bordered by $g,g',g''=12,\cdots,30$, while most of the components that have absolute values greater than 1000.0 are located on the three edges of the cube.

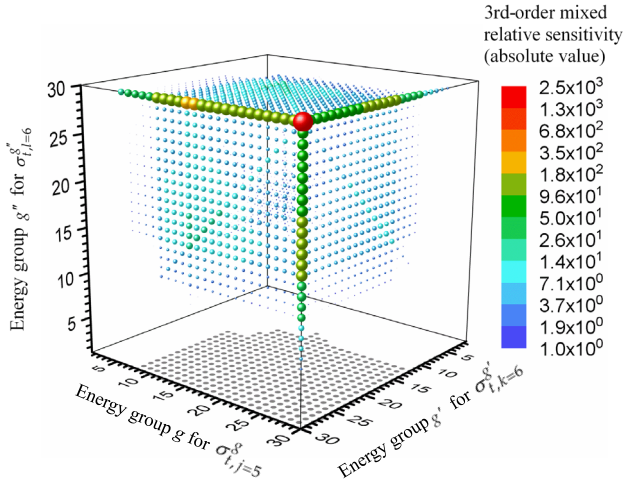

Figure 14. The matrix of sensitivities $\boldsymbol{S}^{(3)}\left(\sigma_{t,\,j=5}^{g},\sigma_{t,\,k=6}^{g'},\sigma_{t,\,l=6}^{g''}\right)$, $g,g',g''=1,\cdots,30$; only elements having absolute values greater than 1.0 are depicted.

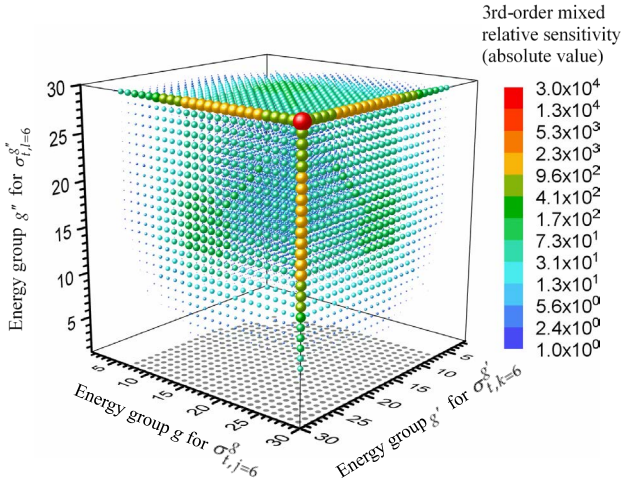

Figure 15. The matrix of sensitivities $\boldsymbol{S}^{(3)}\left(\sigma_{t,\,j=6}^{g},\sigma_{t,\,k=6}^{g'},\sigma_{t,\,l=6}^{g''}\right)$, $g,g',g''=1,\cdots,30$; only elements having absolute values greater than 1.0 are depicted.

4. Summary and Conclusions

This work has presented the numerical computation of the $(180)^3$ third-order mixed sensitivities $\partial^3 L / \partial\sigma_{t,j}^{g}\partial\sigma_{t,k}^{g'}\partial\sigma_{t,l}^{g''}$, $j,k,l = 1,\cdots,6;\ g,g',g'' = 1,\cdots,30$ of the PERP benchmark's total leakage response with respect to the benchmark's 180 microscopic total cross sections. The *largest* magnitudes attained by the 1st-, 2nd- and 3rd-order relative sensitivities of the PERP benchmark's leakage response with respect to the microscopic total cross sections, are summarized in **Table 16**, underscoring the finding that the total number of 3rd-order relative sensitivities that have large values (greater than 1.0) is significantly higher than the number of large 1st- and 2nd-order sensitivities.

Table 16 indicates that the absolute value of the largest 3rd-order relative sensitivity is ca. 437 times larger than the largest 2nd-order sensitivity and is ca. 20,000 times larger than the largest 1st-order sensitivity. All of the largest 1st-, 2nd- and 3rd-order sensitivities involve the microscopic total cross section for the lowest (30th) energy group of isotope ^{1}H (*i.e.*, $\sigma_{t,6}^{30}$). The largest unmixed 3rd-order sensitivity is also with respect to $\sigma_{t,6}^{30}$, namely $S^{(3)}\left(\sigma_{t,6}^{g=30},\sigma_{t,6}^{g'=30},\sigma_{t,6}^{g''=30}\right) = -2.966\times10^4$, as presented in Table 6. However, the largest overall 3rd-order sensitivity is the mixed 3rd-order sensitivity $S^{(3)}\left(\sigma_{t,1}^{g=30},\sigma_{t,6}^{g'=30},\sigma_{t,6}^{g''=30}\right) = -1.88\times10^5$, which also involves the microscopic total cross section for the 30th energy group of isotope ^{239}Pu (*i.e.*, $\sigma_{t,1}^{g=30}$).

The following conclusions can be drawn from the results reported in this work:

1) For all isotopes contained in the PERP benchmark, all of the 1st-order and 3rd-order unmixed relative sensitivities of the PERP's leakage response to the PERP's microscopic total cross sections are negative, while all the unmixed 2nd-order ones are positive.

2) The properties of the unmixed sensitivities for the isotopes contained in the PERP benchmark have been discussed in Section 2, in conjunction with the numerical results presented in Tables 1-6 and will therefore not be repeated here.

3) The number of 3rd-order mixed relative sensitivities that have large values (and are therefore important) is far greater than the number of important 2nd- and 1st-order sensitivities. All of the important 3rd-order mixed relative sensitivities have negative values.

Table 16. Summary of the large relative sensitivities for the PERP benchmark.

	$S^{(1)}(\sigma_t)$	$S^{(2)}(\sigma_t,\sigma_t)$	$S^{(3)}(\sigma_t,\sigma_t,\sigma_t)$
Number of elements with absolute values between 1.0 and 10.0	8	665	45,970
Number of elements with absolute values between 10.0 and 100.0	0	54	11,861
Number of elements with absolute values > 100.0	0	1	1199
Largest relative sensitivity	$S^{(1)}\left(\sigma_{t,6}^{30}\right) = -9.366$	$S^{(2)}\left(\sigma_{t,6}^{30},\sigma_{t,6}^{30}\right) = 429.6$	$S^{(3)}\left(\sigma_{t,1}^{30},\sigma_{t,6}^{30},\sigma_{t,6}^{30}\right) = -1.88\times10^5$

4) Most of the 3rd-order mixed relative sensitivities that involve the microscopic total cross sections of isotopes ^{240}Pu, ^{69}Ga, and ^{71}Ga have values of the order of 10^{-2} or less. However, many 3rd-order mixed relative sensitivities involving the microscopic total cross sections of isotopes ^{239}Pu, C, and ^{1}H have large values.

5) The largest 1st-, 2nd- and 3rd-order sensitivities are $S^{(1)}\left(\sigma_{t,6}^{30}\right)=-9.366$, $S^{(2)}\left(\sigma_{t,6}^{30},\sigma_{t,6}^{30}\right)=429.6$ and $S^{(3)}\left(\sigma_{t,1}^{g=30},\sigma_{t,6}^{g'=30},\sigma_{t,6}^{g''=30}\right)=-1.88\times10^{5}$, respectively. Thus, the largest 1st-, 2nd-order sensitivities are all with respect to the microscopic total cross section for the 30th energy group of isotope ^{1}H (*i.e.*, $\sigma_{t,6}^{30}$), and the largest 3rd-order sensitivity is with respect to the microscopic total cross section for the 30th energy group of isotopes ^{239}Pu and ^{1}H (*i.e.*, $\sigma_{t,1}^{g=30}$ and $\sigma_{t,6}^{30}$). All in all, the microscopic total cross section of isotopes ^{1}H and ^{239}Pu are the two most important parameters affecting the PERP benchmark's leakage response, since they are involved in all of the large 2nd- and 3rd-order sensitivities.

6) The 3rd-order sensitivity analysis presented in this work is the first ever such analysis in reactor physics. The consequences of the results presented in this work on the uncertainty analysis of the PERP benchmark's leakage response will be presented in the accompanying Part III [7].

Conflicts of Interest

The authors declare no conflicts of interest regarding the publication of this paper.

References

[1] Cacuci, D.G. and Fang, R. (2020) Third Order Adjoint Sensitivity and Uncertainty Analysis of an OECD/NEA Reactor Physics Benchmark: I. Mathematical Framework. *American Journal of Computational Mathematics*, **10**, 503-528. https://doi.org/10.4236/ajcm.2020.104029

[2] Valentine, T.E. (2006) Polyethylene-Reflected Plutonium Metal Sphere Subcritical Noise Measurements, SUB-PU-METMIXED-001. In: *International Handbook of Evaluated Criticality Safety Benchmark Experiments*; NEA/NSC/DOC(95)03/I-IX; Organization for Economic Co-Operation and Development; Nuclear Energy Agency, Paris, France.

[3] Cacuci, D.G. (2020) Third Order Adjoint Sensitivity Analysis of Reaction Rate Responses in a Multiplying Nuclear System with Source. *Annals of Nuclear Energy*, **151**, 107924. https://doi.org/10.1016/j.anucene.2020.107924

[4] Cacuci, D.G., Fang, R. and Favorite, J.A. (2019) Comprehensive Second-Order Adjoint Sensitivity Analysis Methodology (2nd-ASAM) Applied to a Subcritical Experimental Reactor Physics Benchmark: I. Effects of Imprecisely Known Microscopic Total and Capture Cross Sections. *Energies*, **12**, 4219. https://doi.org/10.3390/en12214219

[5] Fang, R. and Cacuci, D.G. (2020) Comprehensive Second-Order Adjoint Sensitivity Analysis Methodology (2nd-ASAM) Applied to a Subcritical Experimental Reactor Physics Benchmark: VI. Overall Impact of 1st- and 2nd-Order Sensitivities on Response Uncertainties. *Energies*, **13**, 1674. https://doi.org/10.3390/en13071674

[6] Alcouffe, R.E., Baker, R.S., Dahl, J.A., Turner, S.A. and Ward, R. (2008) PARTISN:

A Time-Dependent, Parallel Neutral Particle Transport Code System. Los Alamos National Laboratory, Los Alamos, NM, USA.

[7] Fang, R. and Cacuci, D.G. (2020) Third Order Adjoint Sensitivity and Uncertainty Analysis of an OECD/NEA Reactor Physics Benchmark: III. Response Moments, *American Journal of Computational Mathematics*, **10**, 559-570. https://doi.org/10.4236/ajcm.2020.104031

Appendix: Mathematical Expression of 3rd-Order PERP Sensitivities

The mathematical expression of the 3rd-order mixed sensitivities $\partial^3 L(\boldsymbol{\alpha})/\partial t_j \partial t_k \partial t_\ell$, $j,k,\ell = 1,\cdots,J_{\sigma t}$ of the PERP leakage response with respect to the group-averaged microscopic total cross sections has been derived in the accompanying Part I [1] and is reproduced below, for convenient reference:

$$\begin{aligned}\frac{\partial^3 L(\boldsymbol{\alpha})}{\partial t_j \partial t_k \partial t_\ell} = -\Big\{&\Big\langle \psi_1^{(3),g}(j,k;r,\boldsymbol{\Omega}), \varphi^g(r,\boldsymbol{\Omega})\Big\rangle_{(1)} \\ &+\Big\langle \psi_2^{(3),g}(j,k;r,\boldsymbol{\Omega}), \psi^{(1),g}(r,\boldsymbol{\Omega})\Big\rangle_{(1)} \\ &+\Big\langle \psi_3^{(3),g}(j,k;r,\boldsymbol{\Omega}), \psi_1^{(2),g}(j;r,\boldsymbol{\Omega})\Big\rangle_{(1)} \\ &+\Big\langle \psi_4^{(3),g}(j,k;r,\boldsymbol{\Omega}), \psi_2^{(2),g}(j;r,\boldsymbol{\Omega})\Big\rangle_{(1)}\Big\}\delta_{g_\ell g} N_{i_\ell,m_\ell},\end{aligned} \tag{1}$$

for $j,k,\ell = 1,\cdots,J_{\sigma t}$,

where

$$\begin{aligned}&\Big\langle \psi_1^{(3),g}(j,k;r,\boldsymbol{\Omega}), \varphi^g(r,\boldsymbol{\Omega})\Big\rangle_{(1)} \\ &= \sum_{g=1}^{G}\int \mathrm{d}V \int_{4\pi} \mathrm{d}\boldsymbol{\Omega}\, \psi_1^{(3),g}(j,k;r,\boldsymbol{\Omega})\varphi^g(r,\boldsymbol{\Omega}),\end{aligned} \tag{2}$$

$$\begin{aligned}&\Big\langle \psi_2^{(3),g}(j,k;r,\boldsymbol{\Omega}), \psi^{(1),g}(r,\boldsymbol{\Omega})\Big\rangle_{(1)} \\ &= \sum_{g=1}^{G}\int \mathrm{d}V \int_{4\pi} \mathrm{d}\boldsymbol{\Omega}\, \psi_2^{(3),g}(j,k;r,\boldsymbol{\Omega})\psi^{(1),g}(r,\boldsymbol{\Omega}),\end{aligned} \tag{3}$$

$$\begin{aligned}&\Big\langle \psi_3^{(3),g}(j,k;r,\boldsymbol{\Omega}), \psi_1^{(2),g}(j;r,\boldsymbol{\Omega})\Big\rangle_{(1)} \\ &= \sum_{g=1}^{G}\int \mathrm{d}V \int_{4\pi} \mathrm{d}\boldsymbol{\Omega}\, \psi_3^{(3),g}(j,k;r,\boldsymbol{\Omega})\psi_1^{(2),g}(j;r,\boldsymbol{\Omega}),\end{aligned} \tag{4}$$

$$\begin{aligned}&\Big\langle \psi_4^{(3),g}(j,k;r,\boldsymbol{\Omega}), \psi_2^{(2),g}(j;r,\boldsymbol{\Omega})\Big\rangle_{(1)} \\ &= \sum_{g=1}^{G}\int \mathrm{d}V \int_{4\pi} \mathrm{d}\boldsymbol{\Omega}\, \psi_4^{(3),g}(j,k;r,\boldsymbol{\Omega})\psi_2^{(2),g}(j;r,\boldsymbol{\Omega}).\end{aligned} \tag{5}$$

The forward multigroup neutron fluxes $\varphi^g(r,\boldsymbol{\Omega})$ are the solutions [1] [4] [5] of the following multigroup transport equation with a spontaneous fission source:

$$B^g(\boldsymbol{\alpha})\varphi^g(r,\boldsymbol{\Omega}) = Q^g(r),\ g = 1,\cdots,G, \tag{6}$$

$$\varphi^g(r_d,\boldsymbol{\Omega}) = 0,\ \boldsymbol{\Omega}\cdot\boldsymbol{n} < 0,\ g = 1,\cdots,G, \tag{7}$$

where r_d is the radius of the PERP sphere, and where

$$\begin{aligned}&B^g(\boldsymbol{\alpha})\varphi^g(r,\boldsymbol{\Omega}) \triangleq \boldsymbol{\Omega}\cdot\nabla\varphi^g(r,\boldsymbol{\Omega}) + \Sigma_t^g(\boldsymbol{\alpha};r)\varphi^g(r,\boldsymbol{\Omega}) \\ &-\sum_{g'=1}^{G}\int_{4\pi}\mathrm{d}\boldsymbol{\Omega}'\varphi^{g'}(r,\boldsymbol{\Omega}')\Big[\Sigma_s^{g'\to g}(\boldsymbol{\alpha};r,\boldsymbol{\Omega}'\to\boldsymbol{\Omega}) + \chi^g(\boldsymbol{\alpha};r)(\nu\Sigma)_f^{g'}(\boldsymbol{\alpha};r)\Big],\end{aligned} \tag{8}$$

$$Q^g(r) \triangleq \sum_{k=1}^{N_f} \lambda_k N_{k,1} F_k^{SF} \nu_k^{SF} \left(\frac{2}{\sqrt{\pi a_k^3 b_k}} \mathrm{e}^{-\frac{a_k b_k}{4}} \right) \int_{E^{g+1}}^{E^g} \mathrm{d}E \, \mathrm{e}^{-E/a_k} \sinh \sqrt{b_k E}. \quad (9)$$

The multigroup adjoint fluxes $\psi^{(1),g}(r,\boldsymbol{\Omega})$ are the solutions of the following 1st-Level Adjoint Sensitivity System (1st-LASS), which has been solved in [4]:

$$A^g(\boldsymbol{\alpha})\psi^{(1),g}(r,\boldsymbol{\Omega}) = \boldsymbol{\Omega}\cdot\boldsymbol{n}\delta(r-r_d), \ g=1,\cdots,G, \quad (10)$$

$$\psi^{(1),g}(r_d,\boldsymbol{\Omega}) = 0, \ \boldsymbol{\Omega}\cdot\boldsymbol{n}>0, \ g=1,\cdots,G. \quad (11)$$

The 2nd-level adjoint fluxes $\psi_1^{(2),g}(j;r,\boldsymbol{\Omega})$ and $\psi_2^{(2),g}(j;r,\boldsymbol{\Omega}), j=1,\cdots,J_{\sigma t}; g=1,\cdots,G$ are the solutions of the following 2nd-Level Adjoint Sensitivity System (2nd-LASS), which have been solved in [4]:

$$A^g(\boldsymbol{\alpha})\psi_1^{(2),g}(j;r,\boldsymbol{\Omega}) = -\delta_{g_j g} N_{i_j,m_j} \psi^{(1),g}(r,\boldsymbol{\Omega}), \ j=1,\cdots,J_{\sigma t}; \ g=1,\cdots,G, \quad (12)$$

$$\psi_{1,j}^{(2),g}(r_d,\boldsymbol{\Omega}) = 0, \boldsymbol{\Omega}\cdot\boldsymbol{n}>0; \ j=1,\cdots,J_{\sigma t}; \ g=1,\cdots,G, \quad (13)$$

$$B^g(\boldsymbol{\alpha})\psi_2^{(2),g}(j;r,\boldsymbol{\Omega}) = -\delta_{g_j g} N_{i_j,m_j} \varphi^g(r,\boldsymbol{\Omega}), \ j=1,\cdots,J_{\sigma t}; \ g=1,\cdots,G, \quad (14)$$

$$\psi_{2,j}^{(2),g}(r_d,\boldsymbol{\Omega}) = 0, \boldsymbol{\Omega}\cdot\boldsymbol{n}<0; \ j=1,\cdots,J_{\sigma t}; \ g=1,\cdots,G. \quad (15)$$

The 3rd-level adjoint fluxes $\psi_1^{(3),g}(j,k;r,\boldsymbol{\Omega})$, $\psi_2^{(3),g}(j,k;r,\boldsymbol{\Omega})$, $\psi_3^{(3),g}(j,k;r,\boldsymbol{\Omega})$ and $\psi_4^{(3),g}(j,k;r,\boldsymbol{\Omega})$ are the solutions of the following 3rd-Level Adjoint Sensitivity System (3rd-LASS) [1]:

$$A^g(\boldsymbol{\alpha})\psi_4^{(3),g}(j,k;\boldsymbol{r},\boldsymbol{\Omega}) = -\psi^{(1),g}(r,\boldsymbol{\Omega})\delta_{g_k g} N_{i_k,m_k}, \ j=1,\cdots,J_{\sigma t}, \ k=1,\cdots,j, \quad (16)$$

$$\psi_4^{(3),g}(j,k;r_d,\boldsymbol{\Omega}) = 0, \ \boldsymbol{\Omega}\cdot\boldsymbol{n}>0, \ j=1,\cdots,J_{\sigma t}, \ k=1,\cdots,j, \quad (17)$$

$$\begin{aligned} &A^g(\boldsymbol{\alpha})\psi_1^{(3),g}(j,k;r,\boldsymbol{\Omega}) \\ &= -\left[\psi_1^{(2),g}(j;r,\boldsymbol{\Omega})\delta_{g_k g} N_{i_k,m_k} + \psi_4^{(3),g}(j,k;r,\boldsymbol{\Omega})\delta_{g_j g} N_{i_j,m_j}\right], \end{aligned} \quad (18)$$

$$\psi_1^{(3),g}(j,k;r_d,\boldsymbol{\Omega},E) = 0, \ \boldsymbol{\Omega}\cdot\boldsymbol{n}>0, \ j=1,\cdots,J_{\sigma t}, \ k=1,\cdots,j, \quad (19)$$

$$B^g(\boldsymbol{\alpha})\psi_3^{(3),g}(j,k;r,\boldsymbol{\Omega}) = -\varphi^g(r,\boldsymbol{\Omega})\delta_{g_k g} N_{i_k,m_k}, \ j=1,\cdots,J_{\sigma t}, \ k=1,\cdots,j, \quad (20)$$

$$\psi_3^{(3),g}(j,k;r_d,\boldsymbol{\Omega}) = 0, \ \boldsymbol{\Omega}\cdot\boldsymbol{n}<0, \ j=1,\cdots,J_{\sigma t}, \ k=1,\cdots,j, \quad (21)$$

$$\begin{aligned} &B^g(\boldsymbol{\alpha})\psi_2^{(3),g}(j,k;r,\boldsymbol{\Omega}) \\ &= -\left[\psi_2^{(2),g}(j;r,\boldsymbol{\Omega})\delta_{g_k g} N_{i_k,m_k} + \psi_3^{(3),g}(j,k;r,\boldsymbol{\Omega})\delta_{g_j g} N_{i_j,m_j}\right], \end{aligned} \quad (22)$$

$$\psi_2^{(3),g}(j,k;r_d,\boldsymbol{\Omega}) = 0, \ \boldsymbol{\Omega}\cdot\boldsymbol{n}<0, \ j=1,\cdots,J_{\sigma t}, \ k=1,\cdots,j. \quad (23)$$

The 3rd-level adjoint fluxes $\psi_3^{(3),g}(j,k;r,\boldsymbol{\Omega})$ and $\psi_4^{(3),g}(j,k;r,\boldsymbol{\Omega})$ are solved first by running the PARTISN-code [6] in forward and adjoint mode, respectively. The adjoint fluxes $\psi_3^{(3),g}(j,k;r,\boldsymbol{\Omega})$ and $\psi_4^{(3),g}(j,k;r,\boldsymbol{\Omega})$ thus computed are subsequently employed, together with previously solved 2nd-level adjoint fluxes $\psi_1^{(2),g}(j;r,\boldsymbol{\Omega})$ and $\psi_2^{(2),g}(j;r,\boldsymbol{\Omega})$ to compute the remaining 3rd-level adjoint fluxes $\psi_1^{(3),g}(j,k;r,\boldsymbol{\Omega})$ and $\psi_2^{(3),g}(j,k;r,\boldsymbol{\Omega})$, respectively. Similarly, $\psi_1^{(3),g}(j,k;r,\boldsymbol{\Omega})$ are computed by running PARTISN [6] in the ad-

joint mode while $\psi_2^{(3),g}(j,k;r,\mathbf{\Omega})$ are computed by running PARTISN [6] in the forward mode. Once all the 3rd-level adjoint fluxes $\psi_1^{(3),g}(j,k;r,\mathbf{\Omega})$, $\psi_2^{(3),g}(j,k;r,\mathbf{\Omega})$, $\psi_3^{(3),g}(j,k;r,\mathbf{\Omega})$ and $\psi_4^{(3),g}(j,k;r,\mathbf{\Omega})$ are obtained, the 3rd-order mixed sensitivities, $\partial^3 L(\boldsymbol{\alpha})/\partial t_j \partial t_k \partial t_\ell$, $j,k,\ell = 1,\cdots,J_{\sigma t}$ are computed by using these fluxes in Equation (1).

Th components t_j, $j = 1,\cdots,J_{\sigma t}$ are defined as follows [1] [4] [5]:

$$\begin{aligned}&\left[t_1,\cdots,t_{J_{\sigma t}}\right]^\dagger \triangleq \left[\sigma_{t,i=1}^1,\sigma_{t,i=1}^2,\cdots,\sigma_{t,i=1}^G,\cdots,\sigma_{t,i}^g,\cdots,\sigma_{t,i=I}^1,\cdots,\sigma_{t,i=I}^G\right]^\dagger,\\ &i = 1,\cdots,I = 6;\ g = 1,\cdots,G = 30;\ J_{\sigma t} = I \times G = 180.\end{aligned} \tag{24}$$

In Equation (24), the dagger denotes "transposition," $\sigma_{t,i}^g$ denotes the microscopic total cross section for isotope *i* and energy group *g*, and $J_{\sigma t}$ denotes the total number of microscopic total cross sections. It is convenient to write the 3rd-order absolute sensitivities of the PERP's leakage response with respect to the microscopic total cross sections as follows:
$\partial^3 L/\partial\sigma_{t,j}^g \partial\sigma_{t,k}^{g'} \partial\sigma_{t,l}^{g''}$, $j,k,l = 1,\cdots,I;\ g,g',g'' = 1,\cdots,G$, for the $I = 6$ isotopes and $G = 30$ energy groups of the PERP benchmark. The matrix
$\partial^3 L/\partial\sigma_{t,j}^g \partial\sigma_{t,k}^{g'} \partial\sigma_{t,l}^{g''}$, $j,k,l = 1,\cdots,I;\ g,g',g'' = 1,\cdots,G$ of 3rd-order absolute sensitivities has dimensions $J_{\sigma t} \times J_{\sigma t} \times J_{\sigma t}\ (= 180 \times 180 \times 180)$, where
$J_{\sigma t} = G \times I = 30 \times 6$. The matrix of 3rd-order *relative* sensitivities, denoted as $\mathbf{S}^{(3)}\left(\sigma_{t,j}^g,\sigma_{t,k}^{g'},\sigma_{t,l}^{g''}\right)$, is defined as follows:

$$\begin{aligned}&\mathbf{S}^{(3)}\left(\sigma_{t,j}^g,\sigma_{t,k}^{g'},\sigma_{t,l}^{g''}\right)\\ &\triangleq \frac{\partial^3 L}{\partial\sigma_{t,j}^g \partial\sigma_{t,k}^{g'} \partial\sigma_{t,l}^{g''}}\left(\frac{\sigma_{t,j}^g \sigma_{t,k}^{g'} \sigma_{t,l}^{g''}}{L}\right),\ j,k,l = 1,\cdots,6;\ g,g',g'' = 1,\cdots,30.\end{aligned} \tag{25}$$